FRACTURE TOUGHNESS OF FRESH WATER ICE AND SALINE ICE

ALI-REZA AZADEH-TEHRANY

FRACTURE TOUGHNESS OF FRESH WATER ICE AND SALINE ICE

by

© Ali-Reza Azadeh-Tehrany, B. Eng.

A Thesis submitted in partial fulfillment
of the requirements for the degree of
Master of Engineering

Faculty of Engineering and Applied Science
Memorial University of Newfoundland

September 1983

St. John's Newfoundland, Canada

To my Parents, Zinath (Fathemeh) and Reza

TABLE OF CONTENTS

ACKNOWLEDGMENTS

The author would like to express appreciation to his Supervisor, Dr. D.B. Muggeridge, for his technical guidance in preparing this thesis and Mr. Austin Bursey for his assistance in the laboratory. The assistance of Mrs. Mary Brown is also acknowledged. The author would also like to thank all members of the Faculty of Engineering and Applied Science of Memorial University for their assistance.

ABSTRACT

The critical stress intensity factor, K_{1C}, of artificially grown fresh water ice was measured by means of a three point bend test on an edge notched rectangular specimen (22.86 cm x 5.08 cm x 2.54 cm) as a function of the cross head speed, grain size, and temperature. The results for fresh water ice showed that K_{1C} increases as the test temperature and cross head speed decreases. The results showed that the grain size has a pronounced effect on the value of the K_{1C}, as the grain size increases so does the value of stress intensity factor (K_{1C}).

A special freezing chamber was designed to produce artificial grown sea ice with a constant brine volume. The critical stress intensity factor, K_{1C}, for artificially grown saline ice was measured at -4°C, -7°C, -11°C, and -20°C for cross head speeds of 2.5 mm/min., 5 mm/min. and 50 mm/min. As for fresh water ice the K_{1C} was strongly dependent on the test temperature, cross head speed, and grain size of the specimen.

Finally the non-linear fracture toughness of saline ice was examined, and the strain energy release rate (G), and the yield stress for each ice specimen was calculated and is reported.

Details of the crystal structure and the Young's modulus for saline ice, together with a theory of non-linear fracture toughness, are presented in the Appendix.

NOMENCLATURE

a	-	crack length
C	-	half the crack length
dC	-	increment of crack extension
du	-	change in strain energy
dw	-	work done by external forces
E	-	Young's modulus
G	-	strain energy release rate
h	-	specimen width
P	-	work associated with plastic and viscous flow
P_Q	-	load of failure
S	-	span length
T	-	traction vector
W	-	strain energy density
y	-	depth of the specimen
z	-	height of the knife edge
γ	-	surface energy
δ	-	corrected crack opening displacement
δ_m	-	measured crack opening displacement
ν	-	Poisson's ratio
σ	-	stress
σ_y	-	yield strength of ice
Γ	-	surface energy

INTRODUCTION

In the last ten years, because of pronounced increase in activities in the Arctic and Antarctic there has been a steady demand for solution of increasingly difficult problems that depend upon a knowledge of mechanical properties of ice (fresh water ice and saline ice). Mechanical properties of ice have been studied extensively by means of compression, bending and shear tests. (The modulus of elasticity of sea ice is presented in the Appendix). However, it is hard to understand the fracture phenomena of ice from those test results, since many crack-like flaws exist in lake ice and sea ice. Therefore linear elastic fracture mechanics, which can deal with substances containing cracks, should be applied to understand the fracture phenomena of ice. Several results of measurements for critical stress intensity factor, K_{1c} are available in the literature for fresh water and sea ice.

In order for K_{1c} to be a valid value, the most important restriction is that the size of the plastically deformed volume in the vicinity of a crack tip should be smaller than any dimension of the specimen. If this condition is satisfied, then K_{1c} is a material constant, and it does reveal the proper fracture propagation of ice.

The grain size effect had been examined by different investigators (Hamza and Muggeridge (1979), Urabe and Yoshitake (1980)), consequently the grain size effect should be considered in the experiments.

There also should be a parameter to measure the amount of ductility or visco-elasticity developed in each ice specimen.

1.0 Fracture Toughness

In the last few decades, different researchers have been studying the mechanical properties of fresh water ice and saline ice by means of small scale or full scale tests. The state of the art of this subject has been presented by Weeks and Assur (1967, 1969), Glen (1975), Gold (1977), Schwarz and Weeks (1977).

Recently a few investigators have tried to determine the fracture toughness of ice. This has opened the door for the application of fracture mechanics to ice problems. The technique approaches the ice strength from a more realistic point of view based on the fact that ice in the field contains a large number of randomly oriented cracks. The work by previous investigators like Liu and Loop (1972), Vaudrey (1977), Goodman (1977) and Hamza and Muggeridge (1978, 1983) has shown the need for more work to be done to investigate the effect of the test temperature and the loading rate on fracture toughness, and to determine an adequate parameter which controls the non-linear and viscoelastic fracture toughness of ice.

Although data exist on the nucleation of cracks, and multiple crack interactions in strength tests in ice, (Goodman, D.J., 1979), little information exists on the critical stress required to make a crack of known geometry propagate. The concept of fracture toughness is widely used in the metals literature, but has not yet gained a wide acceptance in the ice literature and so a short outline will be given here.

Comprehensive reviews of fracture toughness can be found in Lawn and Wilshaw (1975), Knott (1973). In a brittle solid, there is a critical stress at which a crack becomes unstable, and propagates. Griffith (1920) first showed, by a simple energy argument, which avoids the need to know the stresses at the crack tip, that the critical stress for a crack of length 2C in an infinite body, with a stress σ, at right angles to the crack plane is obtained by equating the rate of strain energy release to the incremental work done to create new surface. This gives

$$\sigma_C = \left[\frac{2E\Gamma}{\pi C} \right]^{1/2}$$

where Γ is the surface energy, C the half crack length, and E Young's modulus, if the crack is in plane stress (in plane strain E would be replaced by $E(1 - \nu)^2$, where ν is Poisson's ratio). The crack geometry is given in Fig. 1. This expression was successfully used to explain the brittle fracture of glass.

A crack can open in three ways: Faces can be pulled apart by a stress normal to the crack plane (mode I), the faces can be sheared over each other perpendicular to the crack front (mode II), or the faces can be sheared parallel to the crack front (mode III). We are concerned here only with the mode I case, in which case the stresses at the tip of a sharp crack in the linear or elastic approximation are given by:

$$\sigma_{xx} = \frac{K_1}{\sqrt{2\pi r}} \cos(\theta/2)\,[1 - \sin(\theta/2)\,\mathrm{Sin}(3\theta/2)]$$

$$\sigma_{yy} = \frac{K_1}{\sqrt{2\pi r}} \cos(\theta/2)\,[1 + \sin\theta/2)\,\mathrm{Sin}(3\theta/2)]$$

$$\sigma_{xy} = \frac{K_1}{\sqrt{2\pi r}} \sin(\theta/2)\cos(\theta/2)\,\mathrm{Cos}(3\theta/2)$$

and in plane strain

$$\sigma_{zz} = \nu(\sigma_{xx} + \sigma_{yy})$$

and

$$\sigma_{xz} = \sigma_{yz} = 0$$

K_1 the stress intensity factor, is a material constant which scales the local stresses close to the crack, but also depends on the position of the free surfaces (subscript 1 implies mode I opening).

Griffith (1921, 1924) formulated a fracture criterion based on the hypothesis of strain energy release rate. He proposed that cracks start propagating when the strain energy release rate breaches or exceeds a critical value which equals the energy required to form a new surface. Experiments have shown that Griffith's criterion is very good for brittle material. However, these same experiments have shown that there is a need for a modified criterion for ductile materials. Orowan (1950) and Irwin (1948, 1960) have suggested, for ductile and viscous materials, that the work

available for crack propagation, should be equalled to the sum of the surface energy and the work associated with plastic and viscous flow.

i.e. $\frac{dF}{dc} = \frac{dw - du}{dc} = G > (2\gamma + P)$

where

$dF = dw - du$

dw = work done by external forces

du = change in strain energy

G = strain energy release rate

dc = increment of crack extension (original length of crack = 2C)

γ = surface energy

P = work associated with plastic and viscous flow

The strain energy release rate of a cracked body can be always related to the stress intensity factor (Irwin, 1957) as follows:

$$G = \frac{K_{1c}^2}{E} \text{ for plane stress}$$

$$G = \frac{K_{1c}^2 (1 - \nu^2)}{E} \text{ for plane strain}$$

Liu and Loop (1972) have used a compact tensile specimen to determine fracture toughness, and a wedge opening specimen to study crack arrest in fresh water ice.

They studied the effect of rate of loading and test temperature on the fracture toughness. Their results show that K_{1C} increases as test temperature and rate of loading decreases.

A recent study by Goodman (1977) describes the use of three and four point bending specimens and the medium crack formation concept to estimate fracture toughness of fresh water ice.

Vaudrey (1977), and Urabe and Yoshitake (1980) have performed some insitu tests and reported values for the fracture toughness of sea water ice. In experiments done by Vaudrey four point bending specimens were used to study the effect of brine volume on fracture toughness.

The present work is concerned with a program of small scale experiments which is developed in order to determine the fracture toughness of fresh water ice as well as salt water ice in terms of failure (K_{1C}). In both experiments the three point bending compact specimen has been used, the procedure has been proposed in ASTM E-399 (1980) in order to determine the plane strain fracture toughness (K_{1C}).

1.1 Experimental Procedure for Fresh Water Ice

Fresh water ice was grown in a commercially available cold room. This ice was free of air bubbles due to the use of boiled tap water. The ice was grown at -22°C in boxes measuring 61 x 61 x 61 cm. Ice blocks of 15-18 cm thickness were formed in 4 to 5 days.

A separate group of ice blocks was prepared in much the same manner except that the top surface of the water was seeded with natural snow or crushed ice using 1.18 x 1.18 mm screen. For different ice grain sizes different screens were used. Specimens (22.86 cm x 5.08 cm x 2.54 cm) were cut from the blocks by means of a band saw. The samples were cut so that the direction of growth was perpendicular to the 22.86 cm x 2.54 cm face. Fig. (2) shows the configuration of the specimen relative to the freezing boxes. A layer approximately 6.0 cm thick was always removed from the top of the block in order to make sure that the specimen does not include part of the initial layer made up of grains having randomly oriented c-axis.

Grain size was determined from thin sections cut from the ice blocks. These sections were frozen on a glass plate and their thickness reduced to about 1 mm using a microtome machine. These final thin sections were then examined and photographed under polarized light, (Fig. 3). The grain sizes were 8 mm in one experiment and 12 mm in another. A bandsaw was used to cut a notch into the specimen. Then the notch was sharpened by use of razor blades. This procedure is according to ASTM (1980) E-399. Notch sharpening by a razor blade was used instead of precracking mentioned in ASTM E-399 (1980). The specimen was left at test temperature at least 24 hours to reach the ambient temperature.

The specimens were loaded by a MTS testing machine whose control console was located outside the cold room. This console was equipped with a plotter which supplied a record of loading history, Fig. (4).

The MTS machine was capable of providing cross head speeds of minimum 12 mm/min. and maximum 1200 mm/min. A typical bend fixture which is in accordance with ASTM E-399 (1980) was used and is shown in Fig. (5).

1.1.1 Discussion and Results

Three conditions have to be met in order to have a valid plane strain value for K_{1c}.

1. The crack length and specimen thickness should be > $2.5\ (K_{1c}/\sigma_y)^2$, where σ_y is the yield strength of ice (in this case fresh water ice). This condition could not be checked accurately because of the fact that σ_y for fresh water ice is not well known. But according to (Liu and Loop, 1972) the 2.54 cm should be adequate for both crack length and specimen thickness.
2. The load-deflection curve should satisfy the criterion mentioned in ASTM E-399 (1980). A typical load deflection curve is shown in Fig. (6).
3. The fracture appearance of each specimen should indicate a plane-strain mode of failure. A typical fracture appearance of one of the specimen is shown in Fig. (7). The value of K_{1c} for columnar fresh water ice was determined at temperature of -4°C and -21°C. At each temperature cross head speeds

of 0.1, 0.4 and 3.6 mm/min. were used. The values of K_{1c} were calculated using the following formula (ASTM, E-399, 1980).

$$K_{1c} = \frac{P_Q \cdot S}{By^{3/2}} \cdot Y$$

where

$$Y = 2.9R^{1/2} - 4.6R^{3/2} + 21.8R^{5/2} - 37.6R^{7/2} + 38.7R^{9/2}$$

$$R = \frac{a}{w}$$

a = crack length, mm

y = depth of specimen, mm

B = thickness of specimen, mm

S = span length, mm

P_Q = load of failure, N

Values of K_{1c} are tabulated in table (1) and plotted in Figs. (8,9) for three test temperatures and three rates of loading. These data show that the value of K_{1c} increases as the temperature decreases, and also as the rate of loading decreases the value of K_{1c} increases. This reflects the viscoelastic property of ice under low rates of loading. Figs. (8,9) are the K_{1c} vs rate of loading, the results are compared with those of Hamza and Muggeridge. Fig. (10) is the K_{1c} values vs test temperature.

1.2 Laboratory Preparation of Artificial Saline Ice

Our understanding of the details of the variations in the physical and chemical properties of sea ice is largely based on studies of artificially grown sea ice. There are several reasons for this, the most important of which is that natural sea ice is very difficult to store with the occurrence of significant brine drainage. This brine drainage results in changes in the original ice properties that are usually undesirable. Additional complicating effects that may occur during natural sea ice growth, such as the formation of slush ice and infiltrated snow ice can be avoided in the laboratory. Furthermore, with the laboratory preparation of sea ice, one can control variations in the growth conditions in such a way as to enhance the particular aspect of sea ice that is under study. Finally, it is expensive and many times logistically difficult to send investigators to the field to study sea ice. This is particularly true during the initial period of ice growth when offshore operations usually require either ship or aircraft support. Therefore it is not surprising that the production of artificial sea and salt ice in coldrooms, where the temperature, composition and structure of the ice can be partially controlled, is attractive.

The following is a discussion of a successful technique that has been used to grow artificial sea ice.

1.2.1 Freezing Arrangement

The first requirement in simulating the growth of natural sea ice is to achieve one-directional freezing. Fortunately this is rather easy to accomplish. Figures (11,12) show the freezing chamber that has worked successfully. After the tank was filled with salt water of salinity 15.6 PPT it was placed in a cold room set at a constant temperature (usually -18°C) where it remained until the desired ice thickness was achieved. Both the sides and bottom of the tank were insulated and resistance heating elements were placed within the insulation compartment to cancel out the bottom and side heat losses. In order to achieve a constant brine volume ice from top to the bottom of the chamber, there are three rows of copper pipe located in the bottom of the chamber, Fig. (11). Two rows of these pipes are interconnected and are located in the bottom corners of the chamber. After a layer of approximately 10 cm thick ice is formed on the top of the chamber. This layer of the ice entraps some of the salt contained in the water, and rejects a portion of the salt in the water underlying the frozen layer. Consequently the water underlying the frozen layer of ice is more saline than what it was started with. In order to have a constant brine volume in the ice, the water under the frozen layer should be drawn out of the chamber (this is done by action of the gravity force) and after adjustment of the salinity to the original one. The salinity adjusted water is sent back to

the chamber through the third row of pipes which is located in the middle of the chamber. This return of the water to the chamber has to be done by a water pump. This procedure should be repeated as often as the underlying water shows increase in salinity. The chamber has dimensions 100x90x50 cm, with two perforated plexi-glass sheets dividing the chamber to three interconnected compartments, Fig. (12). After freezing there are three separate ice blocks. The inside walls and bottom floor of the chamber are covered with a live rubber lining. The rubber lining should be lubricated by a lubricant compound for easy removal of the ice.

This special freezing chamber has worked successfully but one has to be careful not to change the original volume of the water in the chamber. A decrease from original volume of the water creates a gap between the frozen layer and the underlying water, which upon freezing causes two or more layers of ice or empty voids which decrease the strength of the ice.

1.3 Plane Strain Fracture Toughness (K_{1c}) of Saline Ice

Natural sea water of 15.6°/$_{oo}$ was obtained from a nearby marine research laboratory centre. This water was placed in a special freezing chamber (refer to freezing arrangement). After the freezing process was successfully done, three separate blocks of ice measuring 90x33x50 cm were obtained from the freezing chamber, Fig. (13). A layer of approximately 15 cm from the top of each ice block was cut and discarded. This procedure was done in order not to have ice of the first and second zone in salt water ice (refer to sea ice structure in Appendix). Also another 10 cm thick layer from the bottom of each ice block was cut and discarded, since the bottom 10 cm layer of ice showed a brine volume higher than the rest of the block. From such ice blocks specimens with dimensions 22.86x 5.08x2.54 cm as mentioned in ASTM E 399 (for the experimental procedure and theory of fracture toughness refer to fracture toughness of fresh water ice), were cut. Grain size was determined from thin sections cut from the ice blocks. These sections were frozen on a glass plate and their thickness was reduced to 1 mm using a microtome machine, Fig. (14). The thin sections were cut all from the third zone of each ice block, and from the top, middle and bottom of each block, Fig. (15, 16, 17), (thin sections from top, middle, bottom of each ice block). Thin sections showed that as the depth of the ice in the block of ice increased, the grain sizes also increased. Overall the grain sizes were from 8 mm for

the top of the ice block to 17 mm at the bottom of each ice block.

After preparation of specimens and determination of grain size, the specimens were tested for determination of the K_{1c} value as it is outlined in ASTM E-399. Since the salt water ice is never in state of equilibrium the thin sections should be examined at the same time as the fracture toughness tests are carried out. The results of the fracture toughness tests and K_{1c} values are tabulated in Table 2.

1.4 Nonlinear Fracture Toughness of Sea Ice

This section of this thesis describes the nonlinear fracture toughness of artificially grown sea ice using a three point bend specimen. The crack opening displacement (COD) was chosen as an adequate parameter to evaluate the amount of ductility and/or viscoelasticity developed in each test specimen. Briefly, K_{1c} is a material parameter which describes the stress required to make a crack of known size propagate. K_{1c} is directly related to the strain energy release rate, G, by the expression (for plane strain)

$$K^2_{1c} = \frac{GE}{1-\nu^2} \qquad (1)$$

where E is the Young's modulus (the Young's modulus of elasticity according to M.P.Langleben for sea ice is a function of brine volume. In Table 3, the Young's modulus for different brine volumes is shown), and ν is Poisson's ratio of the saline ice. For a purely brittle material G is equal 2Γ, where Γ is the surface energy.

The displacement at the crack tip (COD) is related to the "yield stress" in the plastic zone by the expression

$$\delta = K^2_{1c} \frac{(1-\nu^2)}{E} \cdot \frac{1}{\sigma_y} = \frac{G}{\sigma_y} \qquad (2)$$

The crack opening displacement is related to the displacement on the face of the specimen, δ_m, by the expression

$$\delta = \frac{\delta_m}{1+\frac{2.7(a+z)}{h-a}} \qquad (3)$$

where z is the height of the knife edge supporting the gauge above the ice surface, a is the crack length, and h the specimen width.

In this experiment after determination of the K_{1c} value (for calculation of K_{1c} refer to plane strain fracture toughness of freshwater ice in this thesis) and substituting the K_{1c} value into equation (1) the strain energy release rate G for each specimen is found. With help of equation (3) δ the crack opening displacement is found and at last the yield stress of each sample is found by means of equation (2).

Table 3 shows the K_{1c}, clip gauge reading, brine volume, Young's modulus of elasticity, COD, G and σ_y for each test temperature and crosshead speed. There were ten samples tested for each crosshead speed. Table 3 shows only the average value of 10 tests.

Fig. 4(a) shows the attachment of the extensometer to the ice specimen, for measurement of the crack opening displacement. Fig. 21 shows the crack opening displacement as a function of the crosshead speed. As the crosshead speed increases the crack opening displacement decreases.

Fig. 20 shows the crack opening displacement as a function of the test temperature.

DISCUSSION OF THE RESULTS

The standard for valid determination of values of K_{1c}, by ASTM, includes the criterion that

$$B > a > 2.5\left(\frac{K_{1c}}{\sigma_y}\right)^2$$

which ensures the crack length and specimen thickness are within a limited range. After the determination of values of K_{1c} and consequently of σ_y for saline ice, it was noticed that the specimen thickness "B" and crack length "a" would be at least 21 cm which is not a reasonable dimension and is not in the range mentioned by ASTM. Among the specimen sizes recommended by ASTM the 2.54 cm x 5.08 cm x 22.86 cm was chosen since, according to Rolf and Barsom (1977), the plastic zone radius, r_y, in front of a crack is

$$r_y = \frac{1}{6\pi}\left(\frac{K_{1c}}{\sigma_y}\right)^2$$

Thus the relative plastic zone size ahead of a sharp crack is proportional to the value $\left(\frac{K_{1c}}{\sigma_y}\right)^2$ of the specimen. In establishing the specimen size requirements for the K_{1c} test, the specimen dimensions should be large enough compared with the plastic zone, r_y, so that any effect of the plastic zone on the K_{1c} analysis can be neglected. The following calculation shows that for specimens used in the author's experiments, the specimen thickness is approximately 50 times the radius of the plane strain plastic zone size:

$$\frac{\text{specimen thickness}}{\text{plastic zone size}} = \frac{B}{r_y} = \frac{2.5(K_{1c}/\sigma_y)^2}{(1/6\pi)(K_{1c}/\sigma_y)^2} = 47$$

Thus the restriction that the plastic zone be "contained" within an elastic stress field certainly appears to be satisfied.

For saline ice, Vaudrey measured K_{1c} values averaging 72 kPa $m^{\frac{1}{2}}$ for brine volumes of 25-30°/₀₀ at temperatures -10°C and -20°C with a rate of loading of 5.08 mm/min. Urabe and Yoshitake (1981) found that for ice temperatures of -2°C and brine volume of 120°/₀₀ that K_{1c} was related to the grain size of the ice. They found that for ice with grain size equal to 3 mm a value of K_{1c} equal to 50 kPa $m^{\frac{1}{2}}$ and for a grain size of 22 mm, a value of K_{1c} of 75 kPa $m^{\frac{1}{2}}$ and a value of K_{1c} = 100 kPa $m^{\frac{1}{2}}$ for a grain size of 40 mm.

Timco and Frederking (1983) found an average value of 110 kPa $m^{\frac{1}{2}}$ to 140 kPa $m^{\frac{1}{2}}$ for temperatures of -4°C, -7°C, -11°C and -20°C for brine volume ranging from 10 to 55°/₀₀.

The fracture toughness tests performed by the author revealed a minimum value of 78 kPa $m^{\frac{1}{2}}$ at -4°C and a rate of loading of 50 mm/min, and a maximum value of 182 kPa $m^{\frac{1}{2}}$ at -20°C and 2.5 mm/min. rate of loading. The initial grain sizes were from 8 mm from the top of each ice block to 17 mm on the bottom of each ice block. Since there was a 15 cm layer on the top and 10 cm on the bottom of each block that was removed and discarded, consequently the total average grain size, in the remaining block, was around 14 mm. An increase in the ice block depth resulted

in an increase in the grain size, which should be expected from saline ice. In conclusion, the value of K_{1c} increases with decreasing temperature and increasing rate of loading and the value decreases with increasing brine volume and decreasing grain size. Fig. (18) shows K_{1c} as a function of the test temperature and is compared to the results of Goodman and Tabor (1978) and Goodman (1979). Fig. (19) shows K_{1c} as a function of brine volume and shows the results of Timco and Frederking (1983) and Urabe and Yoshitake (1981a). The results found for K_{1c} values are well in agreement with those of other investigators.

Table 3 presents values for G, which is the rate at which energy is released per unit length of crack advance. The following values are those belonging to Liu and Loop (private communication), Goodman and Tabor (1978) and Goodman (1979):

	T °C	K_{1c} kPa $m^{\frac{1}{2}}$	G Jm^{-2}
H.W. Liu and L.W. Loop	-45 to -4	140 to 100	3 to 1
	-12 to -4	177 to 222	3.6 to 5.6
	-12 to -4	123 to 149	1.7 to 2.5
Goodman and Tabor (1978)	-13	116 ± 13	1.5 ± 0.3
	-38	55 to 85	0.5 ± 0.2
The Author	-4	78 - 93	0.79 to 1.12
	-7	90 - 100	0.9 to 1.1
	-11	106-135	1.16 to 1.88
	-20	139 - 182	1.9 to 3.27

The quantity G is essentially a measure of the energy required to propagate a crack in the solid. For the truly brittle solid the stresses generated around the tip of the crack are given by an explicit elastic solution and G is equal to twice the surface energy of the solid. If, however, plastic flow and creep occur at the crack tip, the singularity at the tip is modified. This is the situation with ice and the process becomes more and more complicated as creep deformation becomes more significant. The difference $G-2\Gamma$ is then a measure of the plastic work involved in crack propagation. It can be seen from Table 3 the amount of energy release rate G increases as the temperature decreases. In fact, the increase in G is an indication that at lower temperatures ice behaves in a more brittle fashion and there is less loss of energy due to plastic work.

The yield strength of saline ice for columnar grained S_2 type was from a minimum of 0.22 MPa at -7°C for a crosshead speed of 5.0 mm/min. to 1.8 MPa for -20°C and crosshead speed of 2.5 mm/min., the salinity of specimens was 6.8°/$_{oo}$. Frederking and Timco (1983) reported values of yield strength from 0.415 to 5.22 MPa for ice of slightly less salinity (4.5±5°/$_{oo}$) at a temperature of -35°C. The reason for such high differences between Frederking's and Timco's results and the author's could be attributed to the fact that the salinity and temperature in the experiments of Frederking and Timco were much lower than those in the research by the author. On the other hand, Goodman (1979), in his fracture toughness experiments, found values of σ_y from 0.58 MPa to 0.89 MPa. These values are similar to those found by the author in his experiments.

The yield strength which was found from fracture toughness values (K_{1c}) is the resistance of the ice containing a crack against the application of load perpendicular to the surface of the specimen. This causes compression in the top surface and tension in the cracked surface of the specimen, similar to flexural strength in an uncracked material. The flexural strength reported by Saeki, Ozaki and Kubo for the first year saline ice of the Okhotsk Sea in a three-point experiment was 0.29 MPa (insufficient information is available on salinity, grain size or temperature). The yield strength in the author's experiments are well in agreement with those of Saeki et al.

CONCLUSION

Fracture toughness measurements were successfully completed on artificial fresh water and saline ice. The fracture toughness values, K_{1c}, were obtained from a three point bending test on a notched specimen. The following conclusions are made:

1. The linear elastic-fracture mechanics concept was shown to be applicable for the determination of fracture parameters for fresh water and saline ice.
2. The K_{1c} values for artificial fresh water ice were from 62 KPa $m^{\frac{1}{2}}$ for cross head speeds of 0.1 mm/min., 0.4 mm/min. and 3.6 mm/min. and for temperatures of -4°C and -21°C. The average grain sizes were 9 mm to 10 mm in one experiment and 11 mm to 13 mm in another experiment.
3. The K_{1c} values for artificial saline ice were from 78 KPa $m^{\frac{1}{2}}$ to 182 KPa $m^{\frac{1}{2}}$, for an average grain size of 14 mm, the salinity of ice was 5.8°/$_{oo}$ at temperatures of -4°C, -7°C, -11°C and -20°C. The cross head speeds were 2.5 mm/min., 5 mm/min. and 50 mm/min.
4. The crack opening displacement (COD) was shown to be an adequate parameter to evaluate the amount of ductility and/or viscoelasticity developed in each ice specimen. From COD measurements the energy release rate (G) for each ice specimen found, a minimum value of 0.79 J/m^2 and a maximum value of 3.27 J/m^2 was recorded. Consequently the yield strength of saline ice was found to have a minimum value of 0.24 MPa and

a maximum value of 1.80 MPa. Fracture toughness test was performed for fresh water ice at temperature -4°C and -21°C. The K_{1c} values for fresh water ice are well in agreement with those belonging to Hamza and Muggeridge (1979).

The K_{1c} values for saline ice are well in agreement with those belonging to Vaudrey (1977) and Timco and Frederking (1982) and Goodman (1979). The energy release rate of saline ice G and the yield strength σ_y are compatable with those belonging to Goodman (1979) and Goodman and Tabor (1978).

In further research for determination of ice forces on offshore structures, the solution should be based upon fracture mechanics of ice.

REFERENCES

Assur, (1958), "Growth, Structure and Strength of Sea Ice", U.S. Army Material Command, Cold Regions Research and Engineering Laboratory, Hanover, New Hampshire.

ASTM, (1980), "Standard Test Method for Plane-Strain Fracture Toughness of Metallic Materials", a manual book of ASTM Standards, E-399-74.

Begley, J.A. and Landes, J.D., (1971), Proc. of the National. Symposium on Fracture Mechanics.

Diesburg, D.E., (1974), "Fracture Toughness Test Methods for Abrasion-Resistance White Cast Iron Using Compact Specimen", Fracture Toughness and Slow Stable Cracking, ASTM-STP 559.

Gold, L.W., (1977), "Engineering Properties of Fresh Water Ice", Journal of Glaciology, Vol. 19, No. 81.

Goodman, D.J., (1979), "Critical Stress Intensity Factor (K_{1c}) Measurements at High Loading Rates for Polycrystalline Ice", IUTAM Symposium, Physics and Mechanics of Ice, Copenhagen.

Goodman, D.J. and Tabor, D., (1978), "Fracture Toughness of Ice: A Preliminary Account of Some New Experiments", Journal of Glaciology, Vol. 21, No. 85.

Griffith, A.A., (1921), "The Phenomena of Rupture and Flow in Solids", Phil. Trans. Roy. Soc. London, Ser. A221, pp. 163-198.

Griffith, A.A., (1924), "The Theory of Rupture", Proc. 1st. International Congress for Applied Mechanics, Delft, pp. 55-63.

Hamza, H. and Muggeridge, D.B., (1979), "Fracture Toughness of Fresh Water Ice", Proc. 5th. Intl. Conf. on Port and Ocean Engineering Under Arctic Conditions, Trondheim, Norway.

Hamza, H. and Muggeridge, D.B., (1983), "Non Linear Fracture Toughness of Fresh Water Ice", Proc. 7th. Intl. Conf. on Port and Ocean Engineering Under Arctic Conditions, Helsinki, Vol. 3.

Hutchinson, J.W., (1968), Journal of Mechanics and Physics of Solids, pp. 13-31 and pp. 337-347.

Hobbs, Peter E., (1974), "Ice Physics", Clarendon Press, Oxford.

Irwin, G.R., (1948), "Fracture of Metal", ASTM, Cleveland.

Irwin, G.R., (1957), "Analysis of Stresses and Strains near the End of a Crack Transversing a Plate", U. App. Mech., Vol. 24, No. 3, pp. 361-364.

Irwin, G.R., (1960), "Fracture Mechanics in Structure Mechanics", Pergammon Press, London.

Knott, J.F., (1973), "Fundamental of Fracture Mechanics", Department of Metallurgy and Materials Science, University of Cambridge.

Langleben, M.P., (1962), "Young's Modulus for Sea Ice", Canadian Journal of Physics, Vol. 40, No. 1.

Lawn, B.R. and Wilshaw, T.R., (1975), "Fracture of Brittle Solids", Cambridge University Press.

Liu, H.W. and Loop, W., (1972), (Draft Report), "Fracture Toughness of Fresh Water Ice", CRREL, Hanover, New Hampshire.

Mantis, Homer T., (1951), "Review of the Properties of Snow and Ice", Engineering Experiment Station, Institute of Technology, University of Minnesota.

Michel, B., (1978), "Ice Mechanics", Les Presses de l'Universite Laval, Quebec City.

Orowan, E., (1950), "Fatigue and Fracture of Metals", Proc. MIT Symposium, p. 139.

Paris, P.C., (1977), "Fracture Mechanics in the Elastic-Plastic Regime", Proc. 10th. National Symposium on Fracture Mechanics, ASTM-STP 631.

Peyton, H.R., (1966), "Sea Ice Strength", Geophysical Institute of the University of Alaska.

Pounder, E.R., (1965), "The Physics of Ice", Pergammon Press, Oxford.

Rolfe, S.T. and Barsom, J.M., (1977), "Fracture and Fatigue Control in Structures", Prentice-Hall Inc., Englewood Cliffs, New Jersey.

Saeki, H., Ozaki, A. and Kubo, Y, (1981), "Experimental Study on Flexural Strength and Elastic Modulus of Sea Ice", Proc. 6th. Intl. Conf. on Port and Ocean Engineering Under Arctic Conditions, Quebec, Vol. 1.

Schwartz, J. and Weeks, W.F., (1977), "Engineering Properties of Sea Ice", Journal of Glaciology, Vol. 19, No. 81.

Sih, G.C., (1976), "Fracture Toughness Concept Properties Related to Fracture Toughness", ASTM-STP 605, pp. 3-13.

Timco, G.W. and Frederking, R.M.W., (1982), "Flexural Strength and Fracture Toughness of Sea Ice", Cold Region Science and Technology, Vol. 8, pp. 35-41.

Timco, G.W. and Frederking, R.M.W., (1983), "Uniaxial Compressive Strength and Deformation of Beaufort Sea Ice", 7th. International Conference on Port and Ocean Engineering Under Arctic Conditions, Helsinki, Finland.

Urabe, N. and Yoshitake, A., (1980), "Fracture Toughness of Sea Ice In-Situ Measurement and its Application", Cold Regions Science and Technology, Vol. 3, No. 1, p. 29.

Urabe, N. and Yoshitake, A., (1981a), "Fracture Toughness of Sea Ice In-Situ Measurement and its Application", Proc. 6th. International Conference on Port and Ocean Engineering Under Arctic Conditions, Quebec City, Canada, Vol. 1, pp. 356-365.

Urabe, N. and Yoshitake, A., (1981b), "Strain Rate Dependent Fracture Toughness (K_{1c}) of Pure Ice and Sea Ice", Proc. IAHR Symposium on Ice, Quebec City, Canada, Vol. II, pp. 551-563.

Vaudrey, K.D., (1977), "Ice Engineering, Study of Related Properties of Floating Sea Ice Sheets and Summary of Elastic and Viscoelastic Analysis".

Weeks, W. and Assur, A., (1971), "The Mechanical Properties of Sea Ice", Cold Regions Research and Engineering Laboratory, Hanover, New Hampshire.

TABLE 1

Fracture Toughness of Columnar Freshwater Ice

GRAIN SIZE = 9 ~ 10 mm

Test Temp °C	Cross Head Speed mm/min	K_{1c}(Max) kPa $m^{1/2}$	K_{1c}(Min) kPa $m^{1/2}$	K_{1c}(Ave) kPa $m^{1/2}$	Stand Dev kPa $m^{1/2}$
-4°C	0.1	125.00	87.00	106.20	13.20
	0.4	90.00	50.00	67.50	13.50
	3.6	90.00	50.00	62.30	12.60
-21°	0.1	160.00	112.00	128.60	14.80
	0.4	160.00	82.00	103.90	22.60
	3.6	122.00	83.00	103.30	14.50

GRAIN SIZE = 11 ~ 13 mm

-4°	0.1	327.00	136.00	210.80	56.50
	0.4	302.00	185.00	219.20	38.30
	3.6	164.00	110.00	139.40	21.80
-21°	0.1	480.00	190.00	393.20	103.10
	0.4	300.00	110.00	230.20	63.70
	3.6	187.00	110.00	164.60	24.60

NOTE: THE RESULTS ARE AVERAGES OF A MINIMUM OF 10 TESTS

TABLE 2
Fracture Toughness for Saline Ice
Average grain size = 14 mm

Test Temp °C	Brine Volume °/oo	Cross Head Speed mm/min	Ave Clip Gauge Reading mm	K_{1c} (Max) kPa $m^{1/2}$	K_{1c} (Min) kPa $m^{1/2}$	K_{1c} (Ave) kPa $m^{1/2}$	Stand Dev kPa $m^{1/2}$	K_{1c} (Ave) kPa $m^{1/2} s^{-1}$
-4°	84.5	2.5	0.015	118	58	93	22	19
	84.5	5.0	0.017	116	58	88	24	13
	84.5	50.0	0.011	104	52	78	17	19
-7°	51.3	2.5	0.015	146	47	100	27	16
	51.3	5.0	0.019	131	52	94	27	14
	51.3	50.0	0.011	112	54	90	18	16
-11°	35.1	2.5	0.020	178	62	135	39	20
	35.1	5.0	0.023	154	77	112	22	16
	35.1	50.0	0.012	203	64	106	42	16
-20°	23.0	2.5	0.008	225	160	182	33	28
	23.0	5.0	0.018	248	107	176	47	17
	23.0	50.0	0.021	168	119	139	19	12

NOTE: THE RESULTS ARE AVERAGES OF A MINIMUM OF 10 TESTS

TABLE 3

Fracture Toughness and Energy Release Rate for Saline Ice
Average grain size ≈ 14 mm

Test Temp °C	Brine Volume v_b °/oo	Cross Head Speed mm/min	Clip Gauge Reading mm	Corrected δ mm	K_{1c} kPa $m^{1/2}$	E GPa	G J/m^2	σ_y MPa
-4°C	84.5	2.5	0.015	0.004	93	7.0	1.12	0.32
	84.5	5.0	0.017	0.004	88	7.0	1.00	0.25
	84.5	50.0	0.011	.003	78	7.0	0.79	0.30
-7°	51.3	2.5	0.015	0.004	100	8.2	1.10	0.31
	51.3	5.0	0.019	0.005	94	8.2	0.98	0.22
	51.3	50.0	0.011	0.003	90	8.2	0.90	0.35
-11°	35.1	2.5	0.020	0.005	135	8.8	1.88	0.40
	35.1	5.0	0.023	0.005	112	8.8	1.30	0.24
	35.1	50.0	0.012	0.003	106	8.8	1.16	0.41
-20°	23.0	2.5	0.008	0.002	182	9.2	3.27	1.80
	23.0	5.0	0.018	0.004	176	9.2	3.06	0.73
	23.0	50.0	0.021	0.005	139	9.2	1.90	0.38

NOTE: THE RESULTS ARE AVERAGES OF A MINIMUM OF 10 TESTS ($\nu = 0.3$)

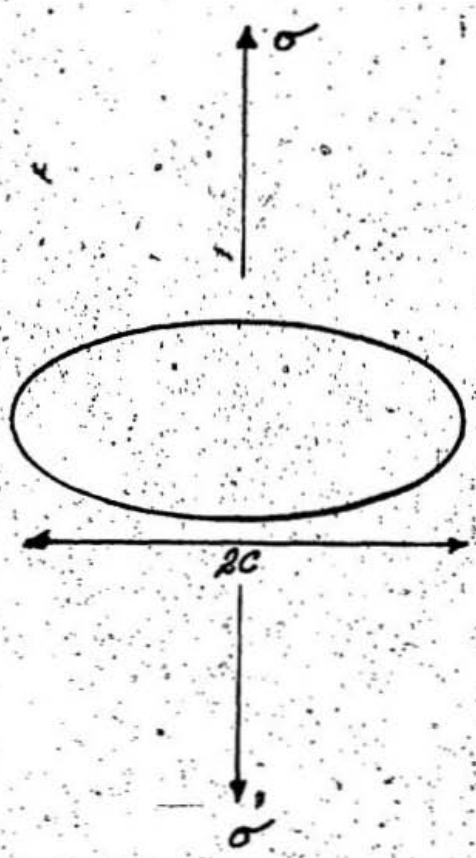

Fig 1 The crack-geometry for Griffth 's calculation

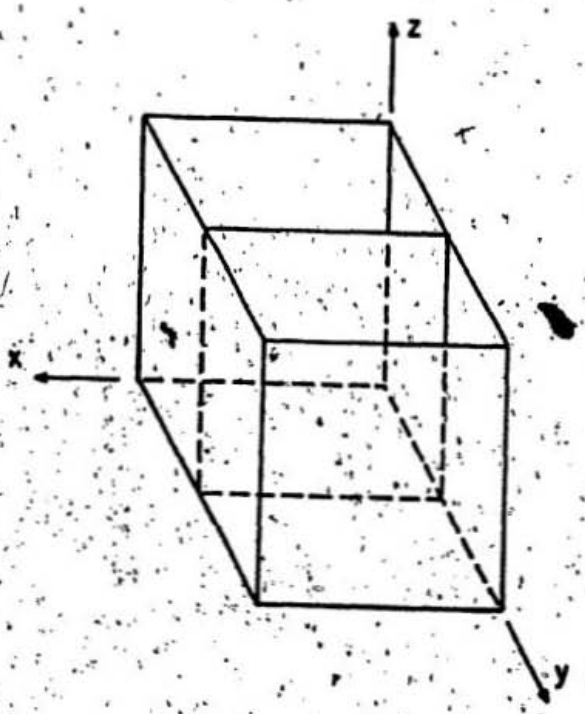

Dim. 60.96 x 60.96 x 60.96 cm

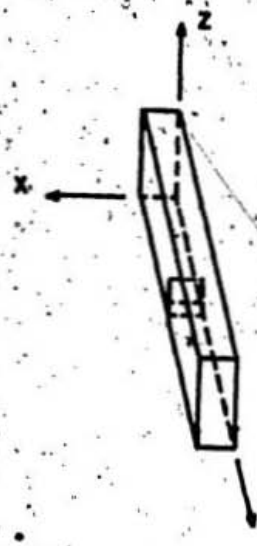

Dim. 22.86 x 5.08 x 2.54 cm

Fig. 2 Specimen geometry

(From Hamza and Muggeridge, 1379)

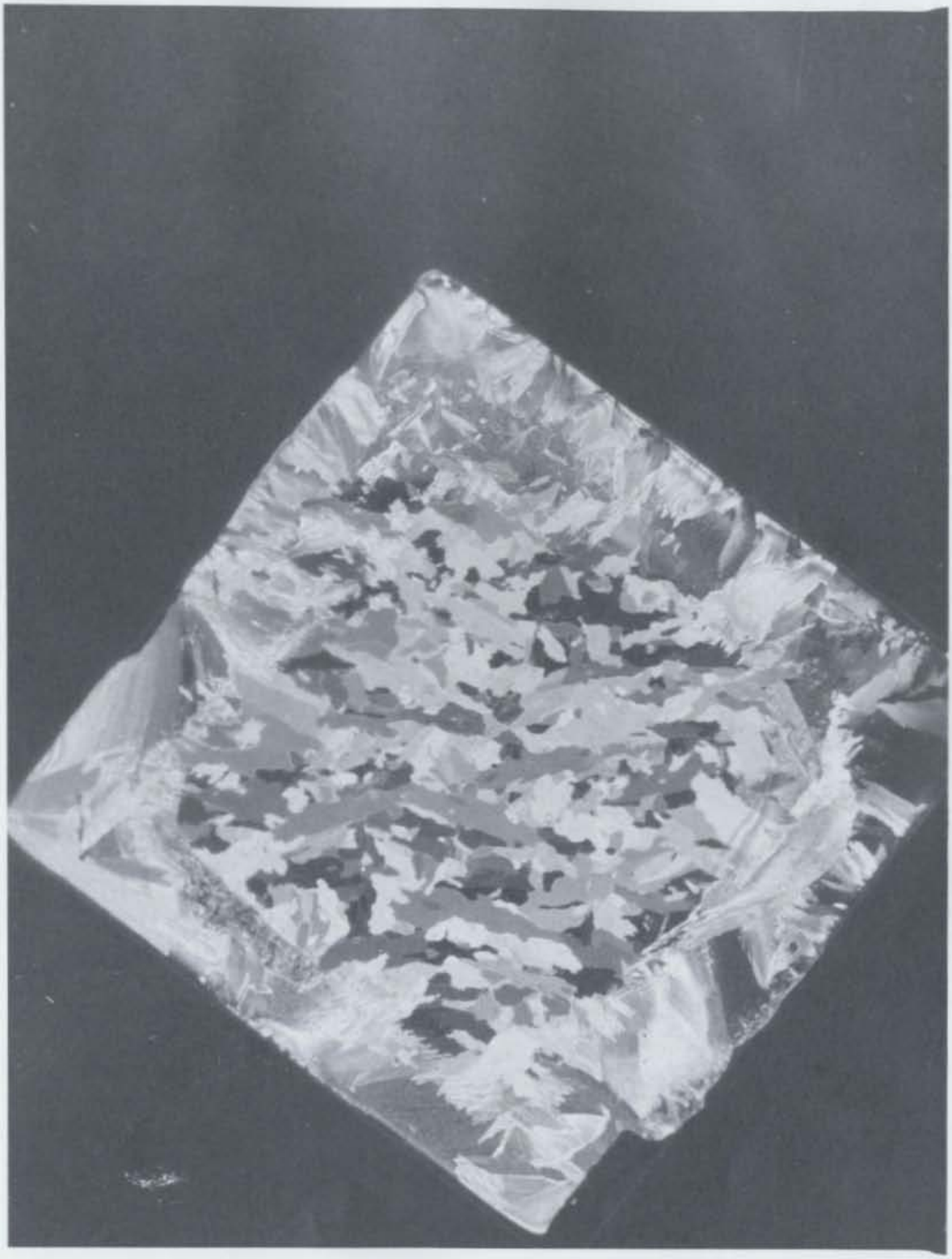

FIGURE 3 Thin Cross-Section

0 10 20 30 40 mm
Scale

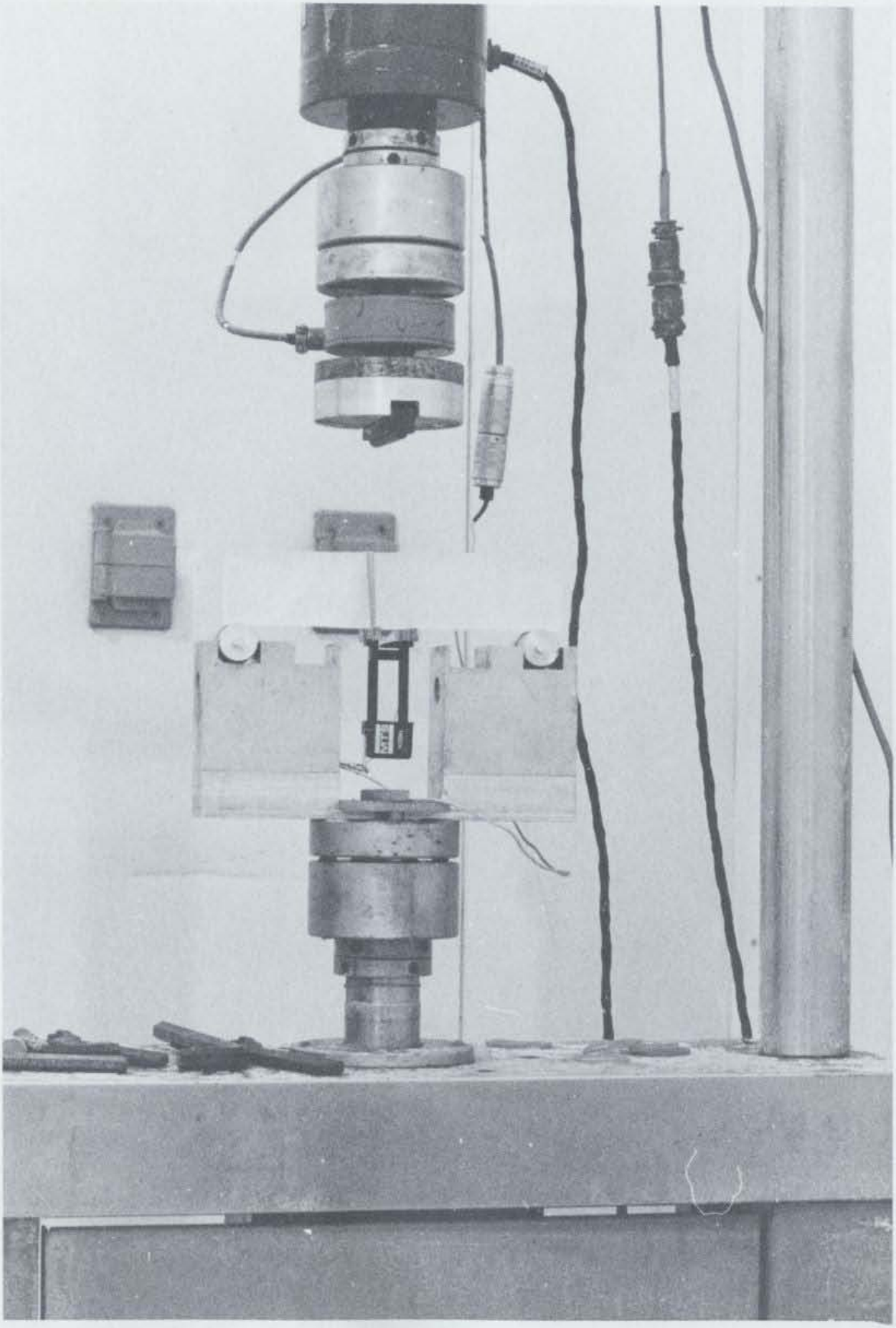

4(a) M.T.S. Machine Inside the Coldroom.

FIGURE 4(b) The Control Console of M.T.S. Machine Outside The Coldroom.

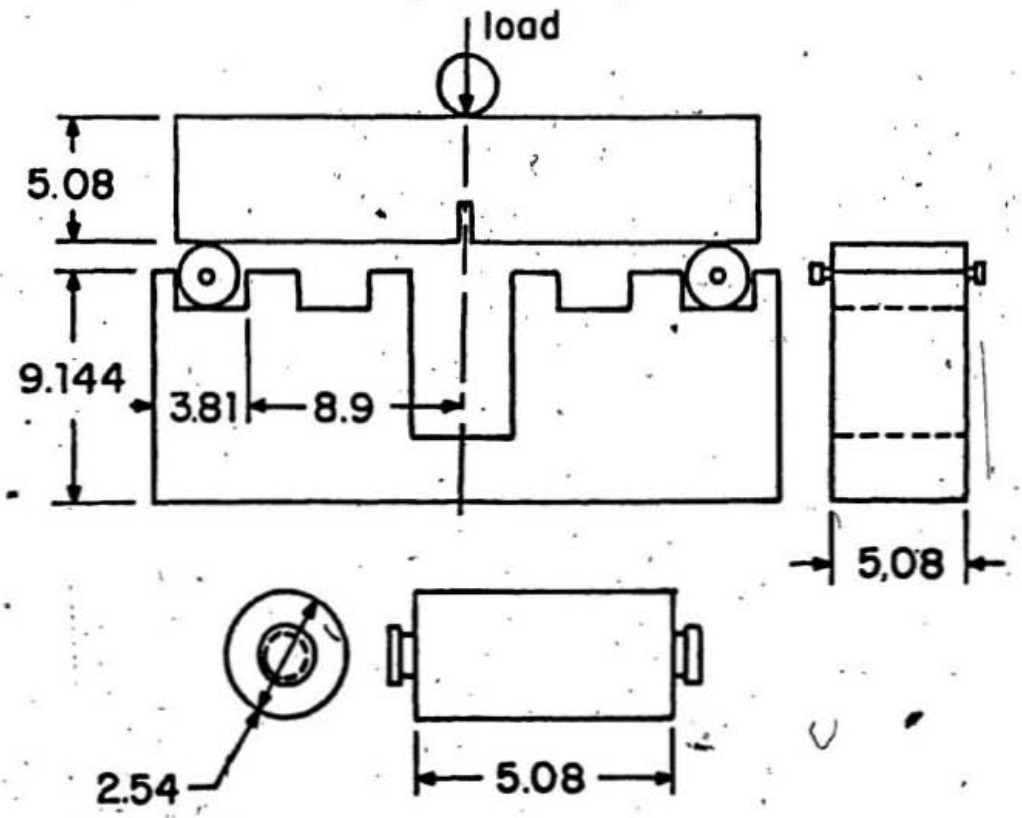

All dimensions in cm.

Fig. 5 Bend test fixture.

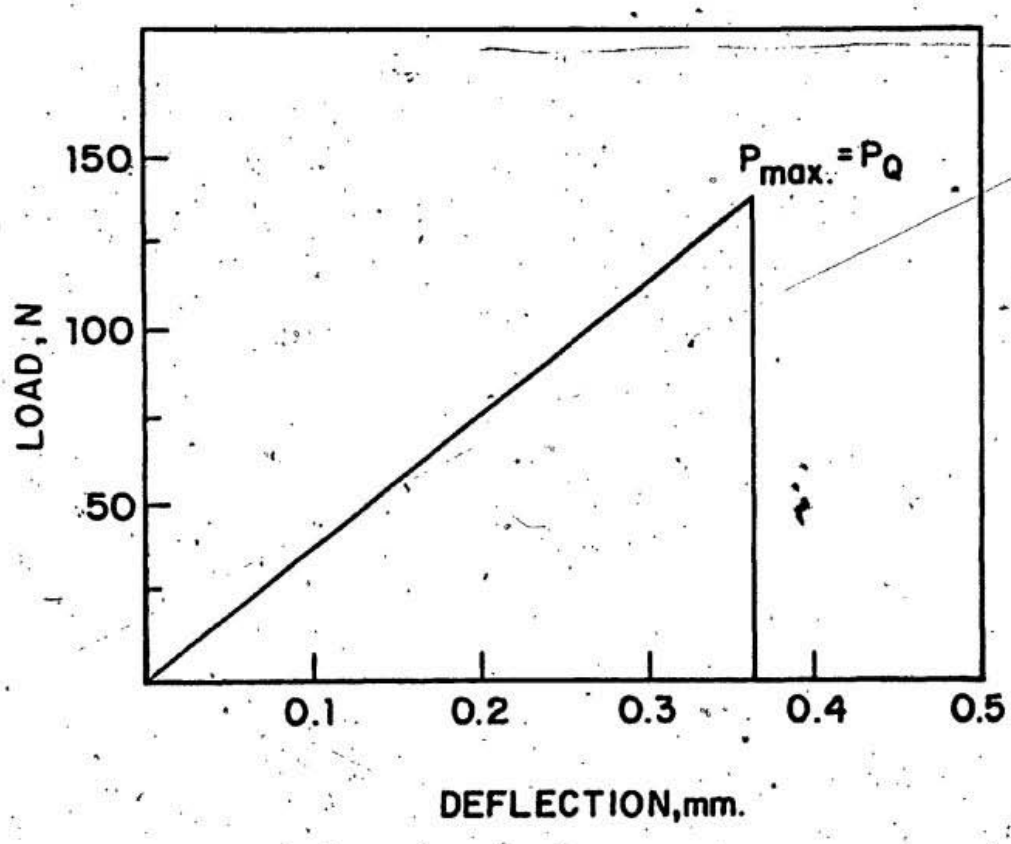

Fig. 6 Typical load deflection curve.
(From Hamza and Muggeridge, 1979)

Fig. 7. Typical Fracture Surface (from Hamza and Muggeridge, 1979)

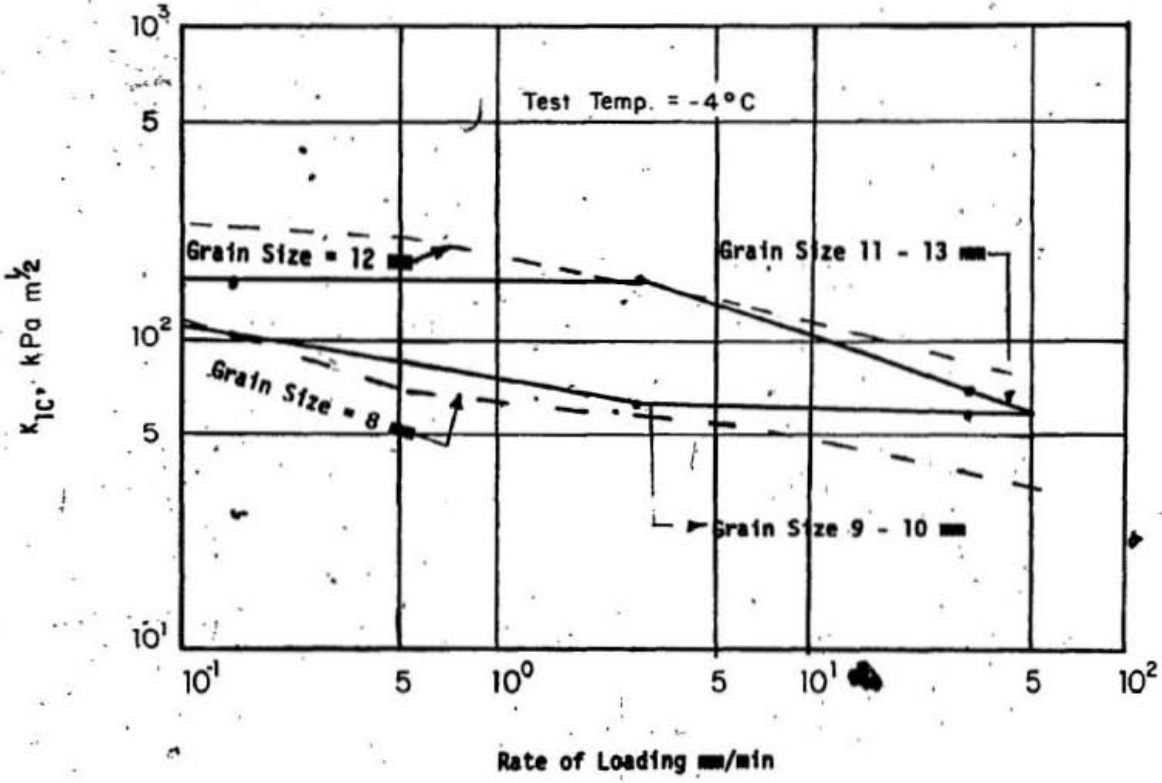

Figure 8 Effect of Grain Size on Fracture Toughness of Columnar Fresh Water Ice

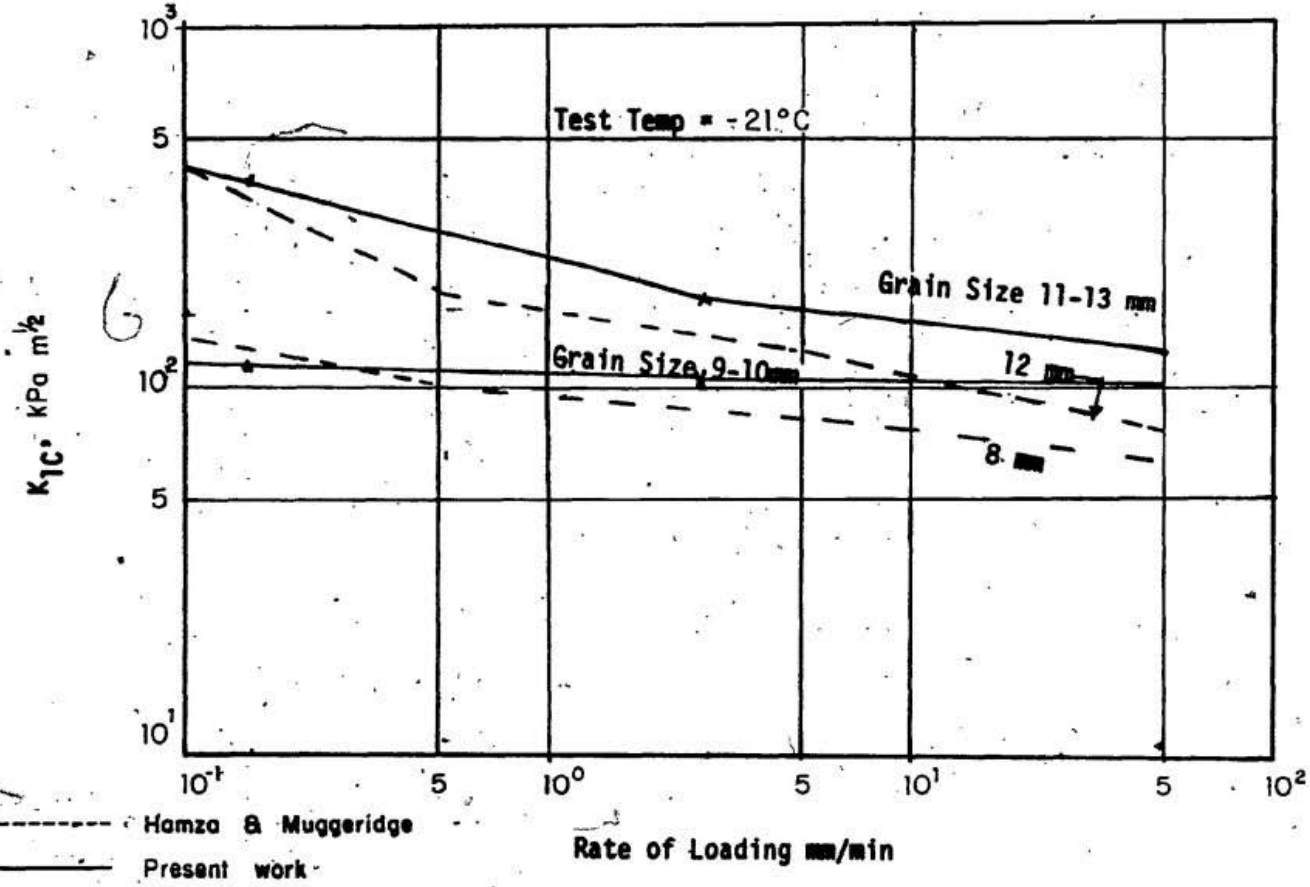

Figure 9 Effect of rate of loading on fracture toughness of columnar fresh water ice.

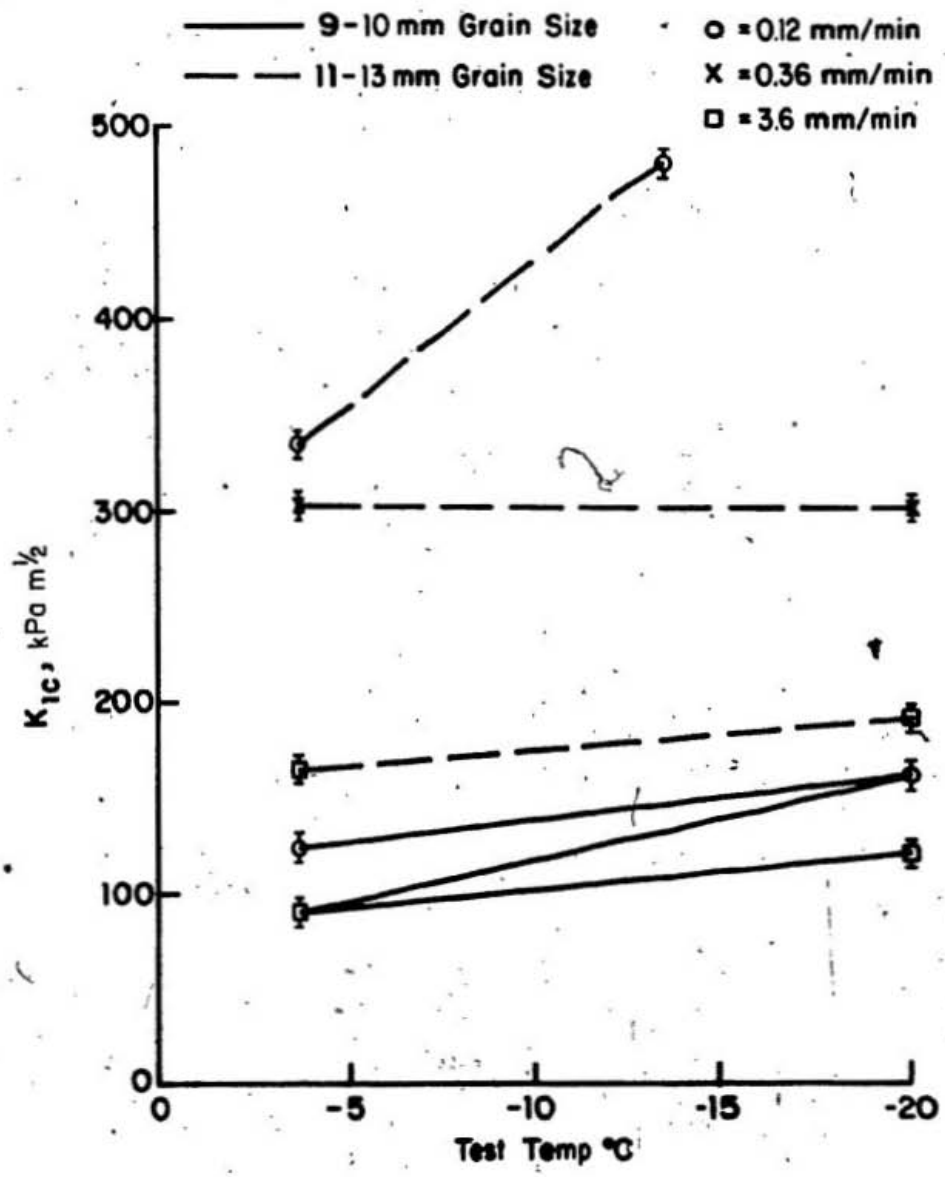

Fig. 10 – Effect of temperature and rate of loading on fracture toughness of columnar fresh water ice.

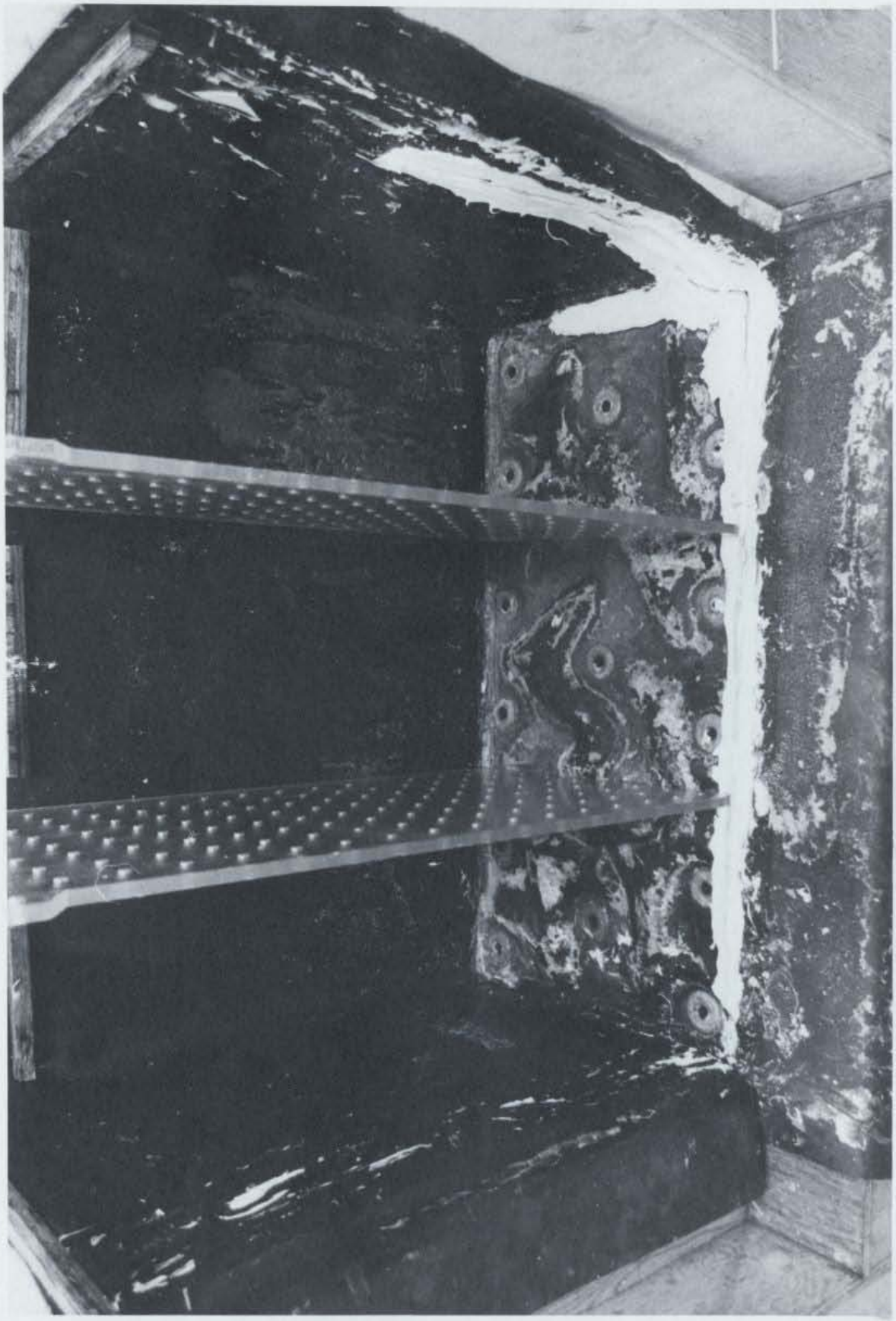

FIGURE 11 Inside The Freezing Chamber.

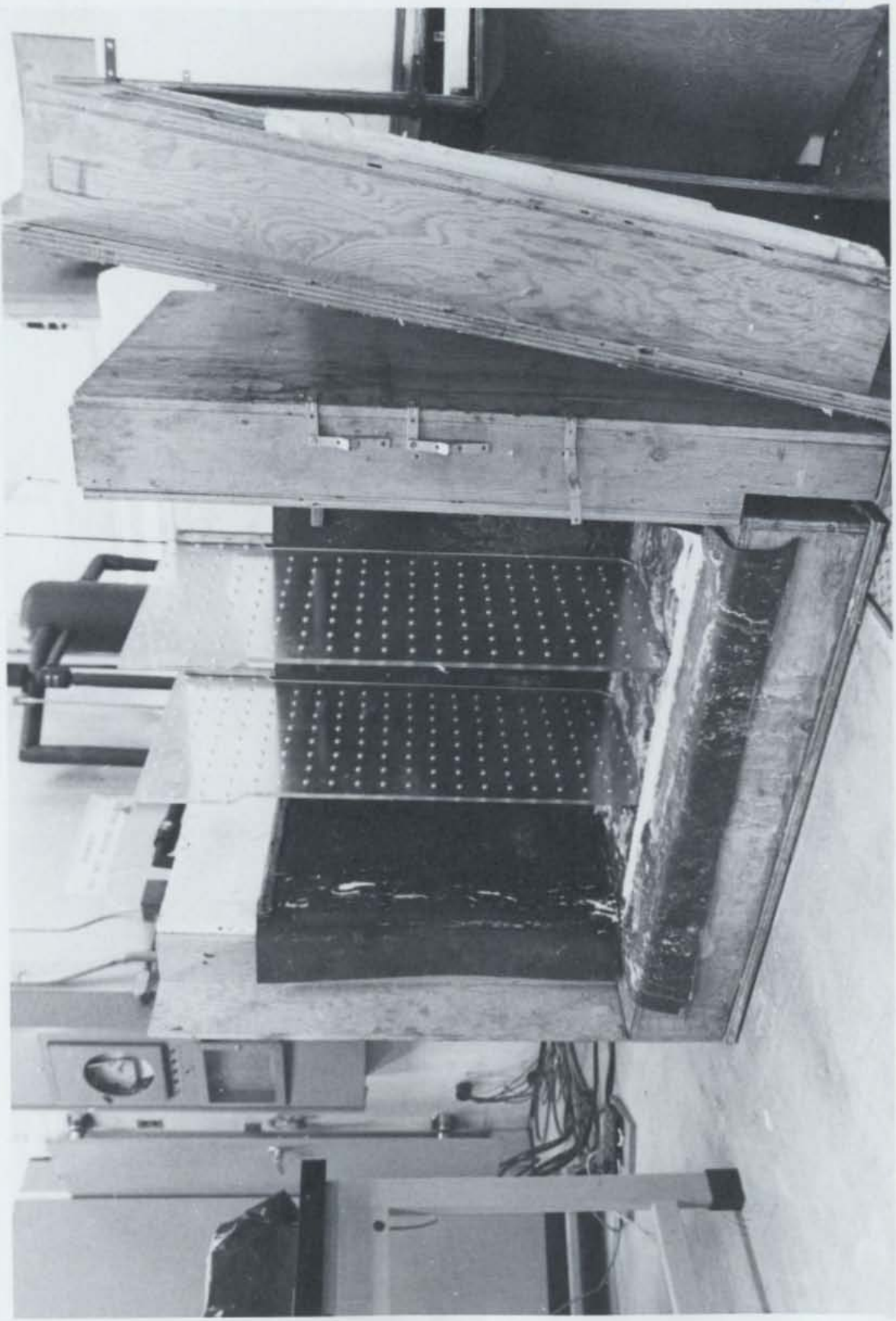

FIGURE 12 The Freezing Chamber.

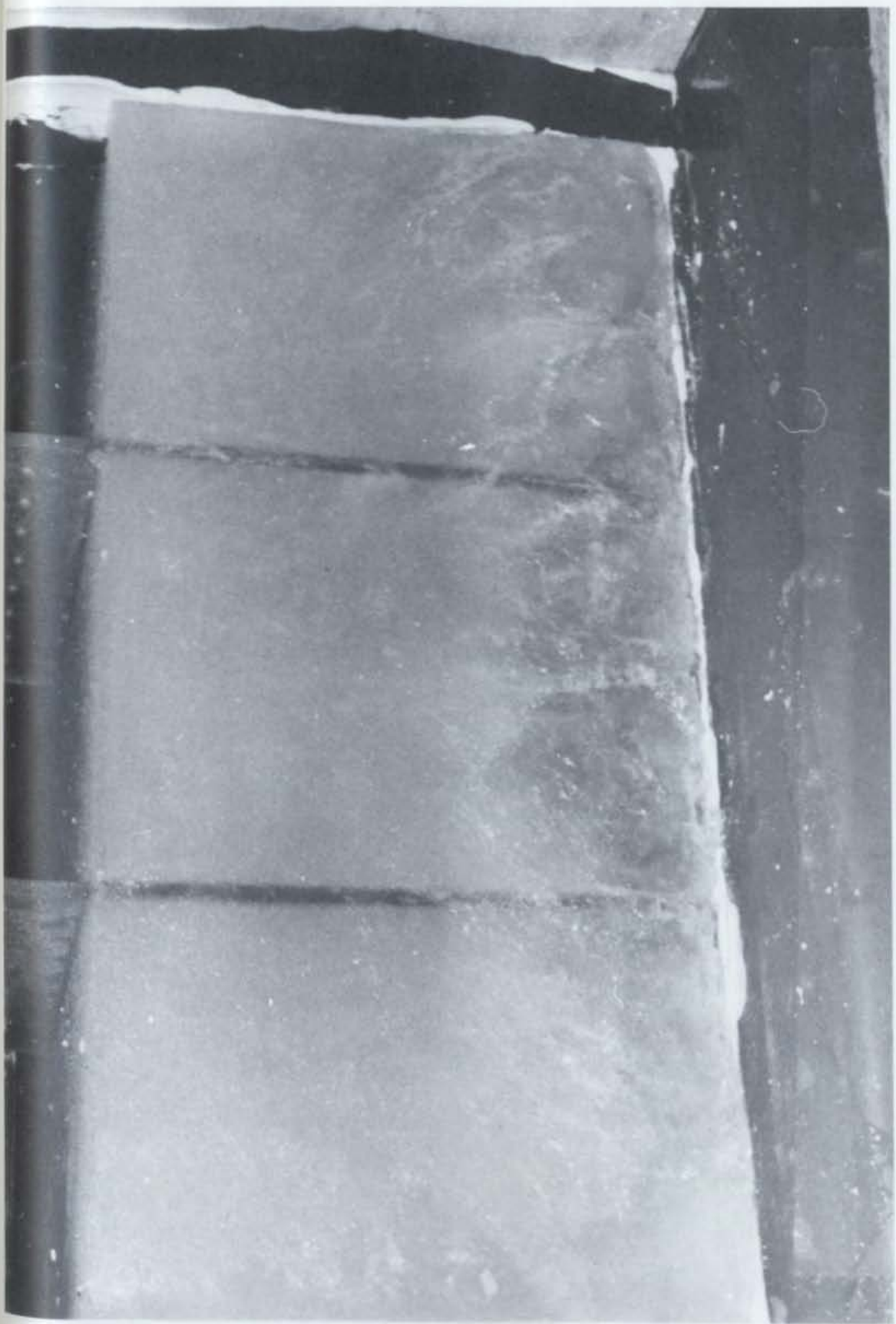

FIGURE 13 - Three Separate Ice Blocks From the Freezing Chamber.

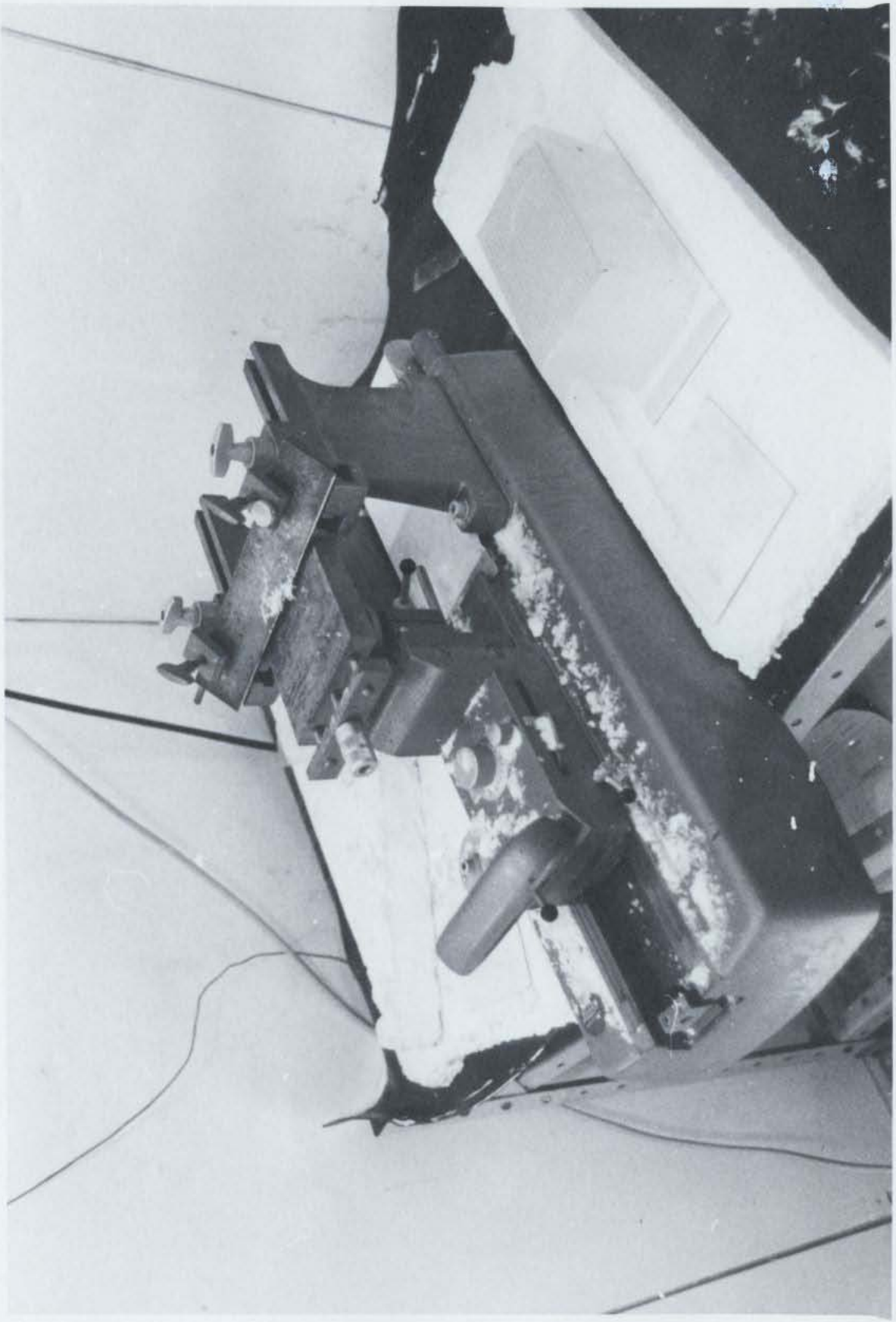

FIGURE 14 - The Microtome Machine.

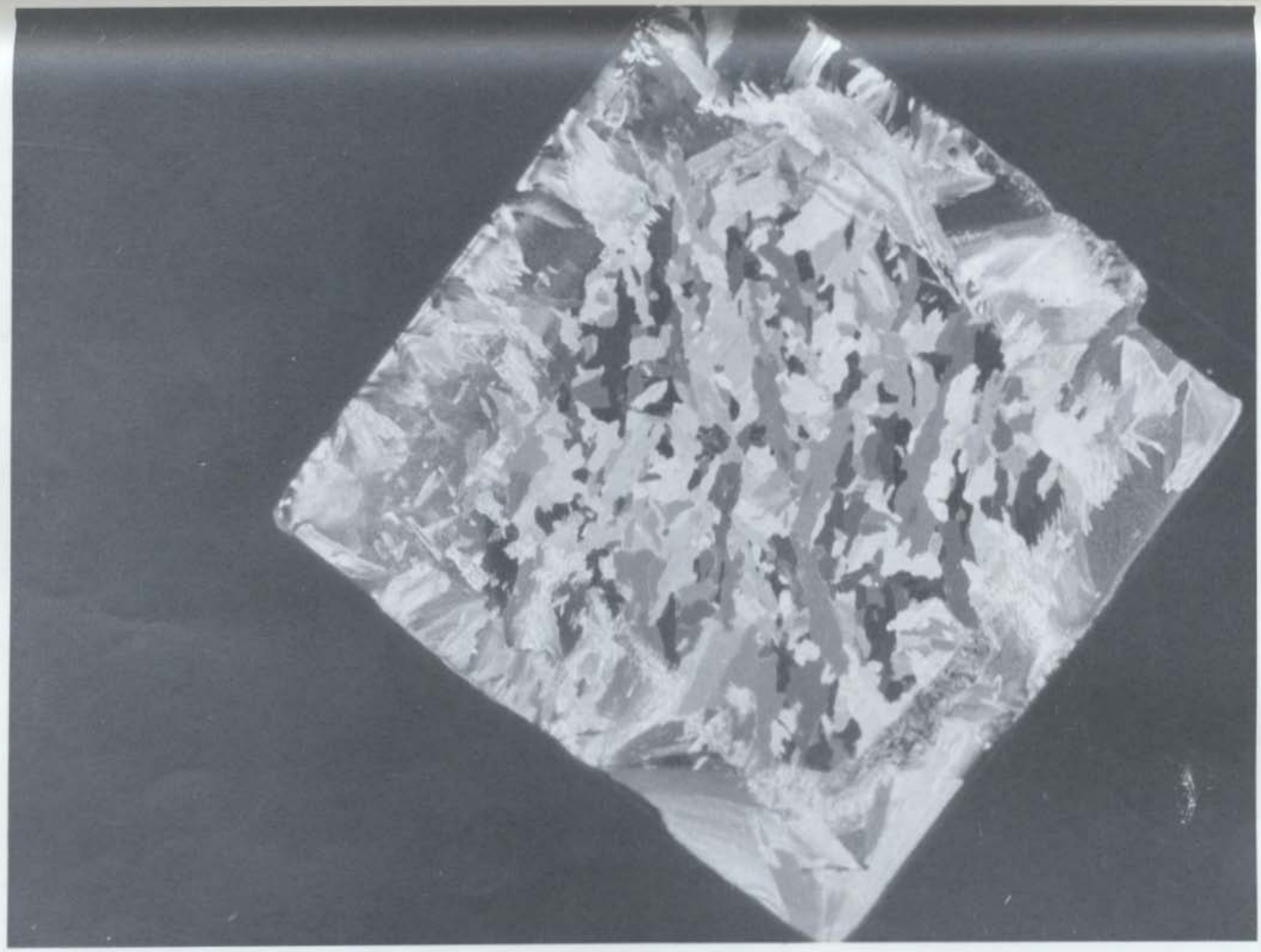

FIGURE 15 - Thin Section From Top of an Ice Block.

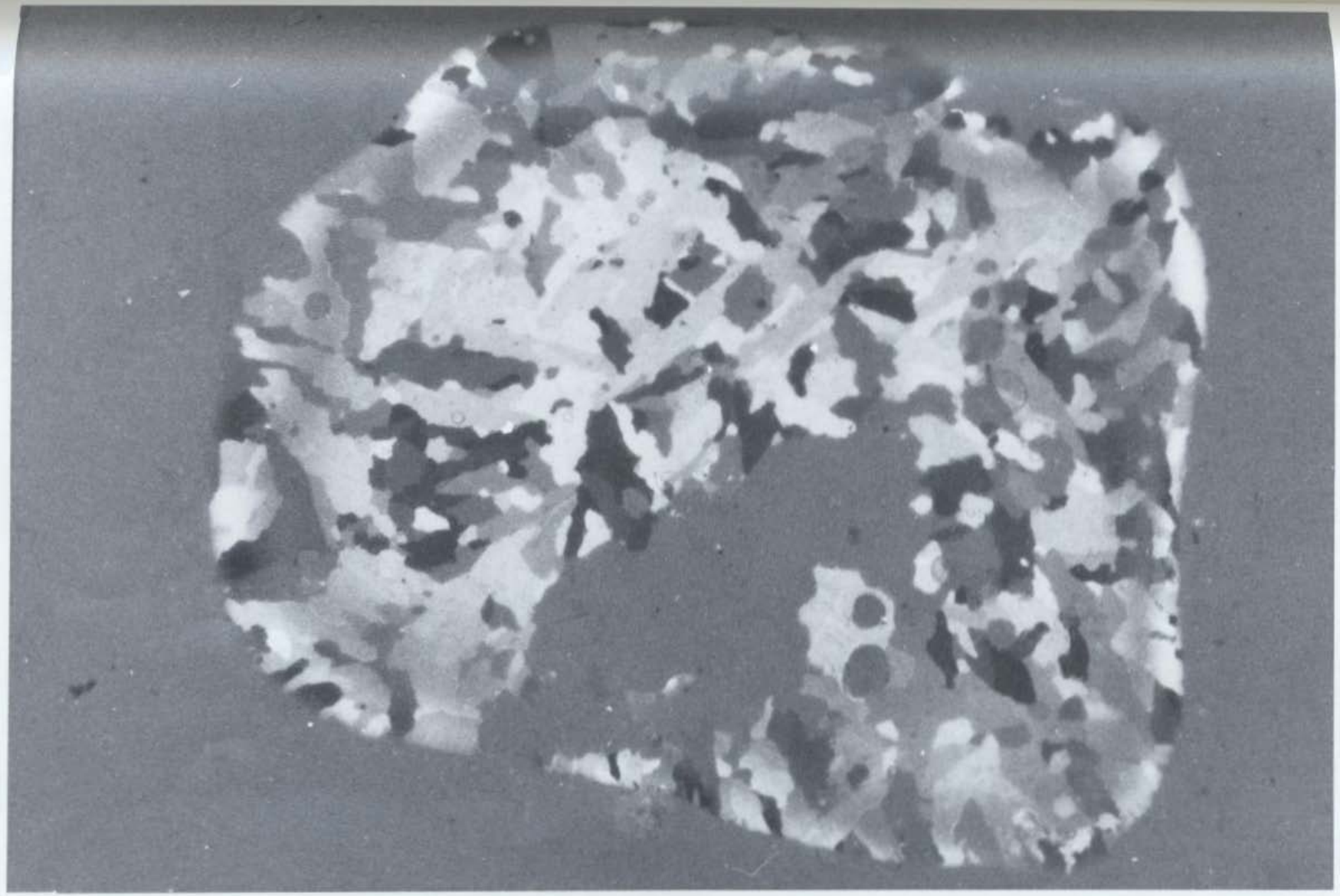

FIGURE 16 - Thin Section From Middle Depth of an Ice Block.

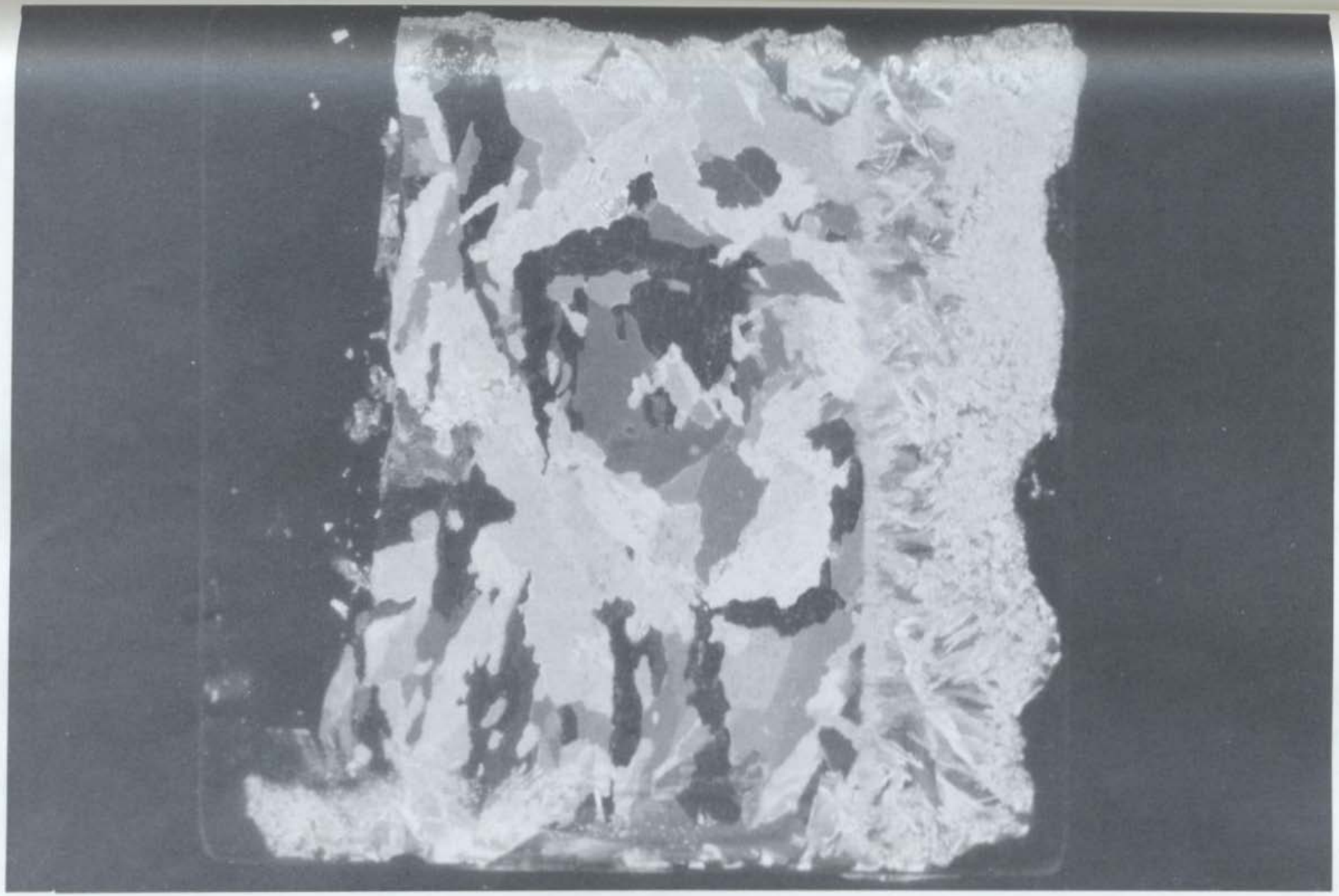

FIGURE 17 - Thin Section from Bottom of an Ice Block.

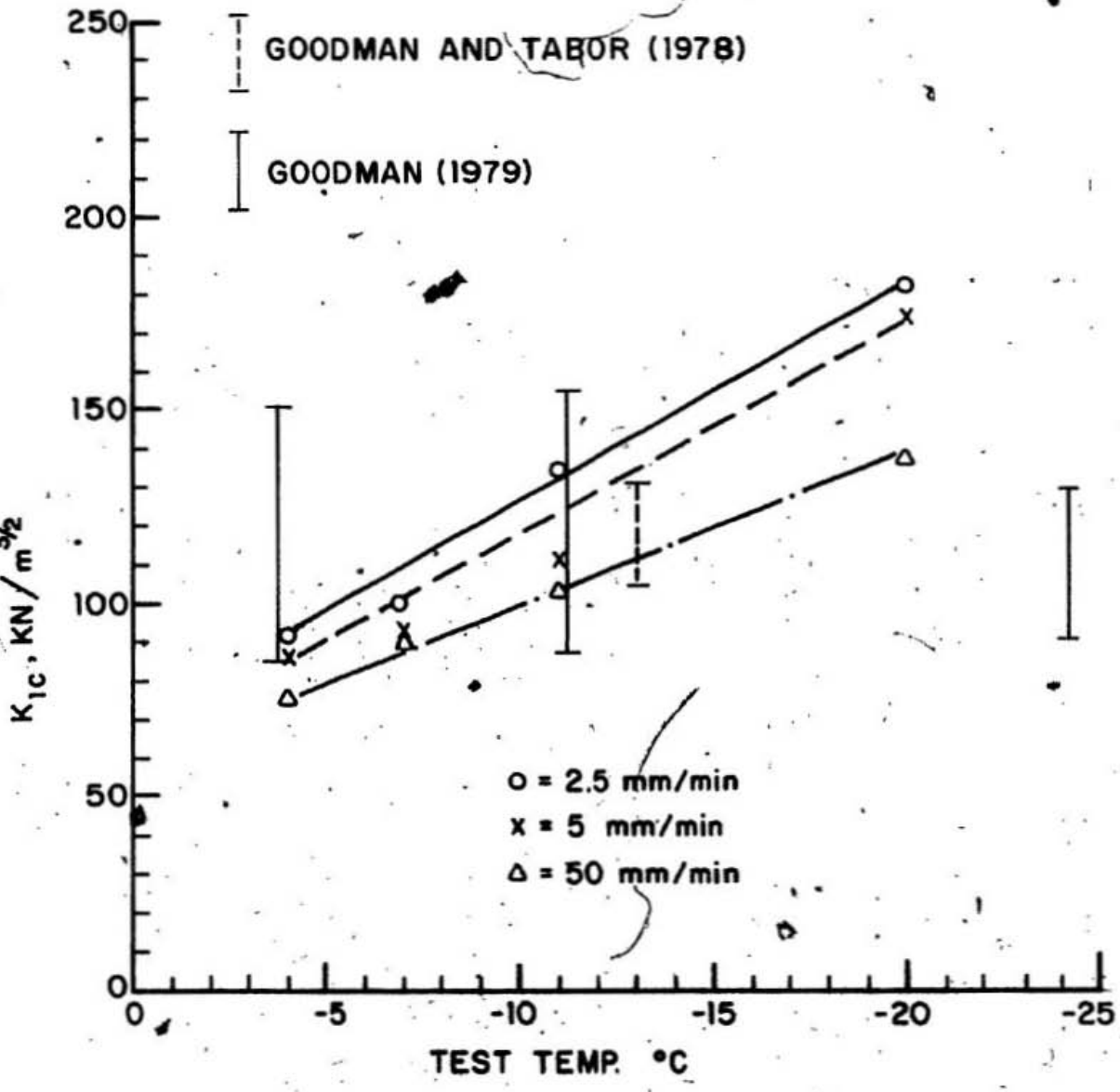

Fig. 18. K_{1C} as a function of Test Temperature

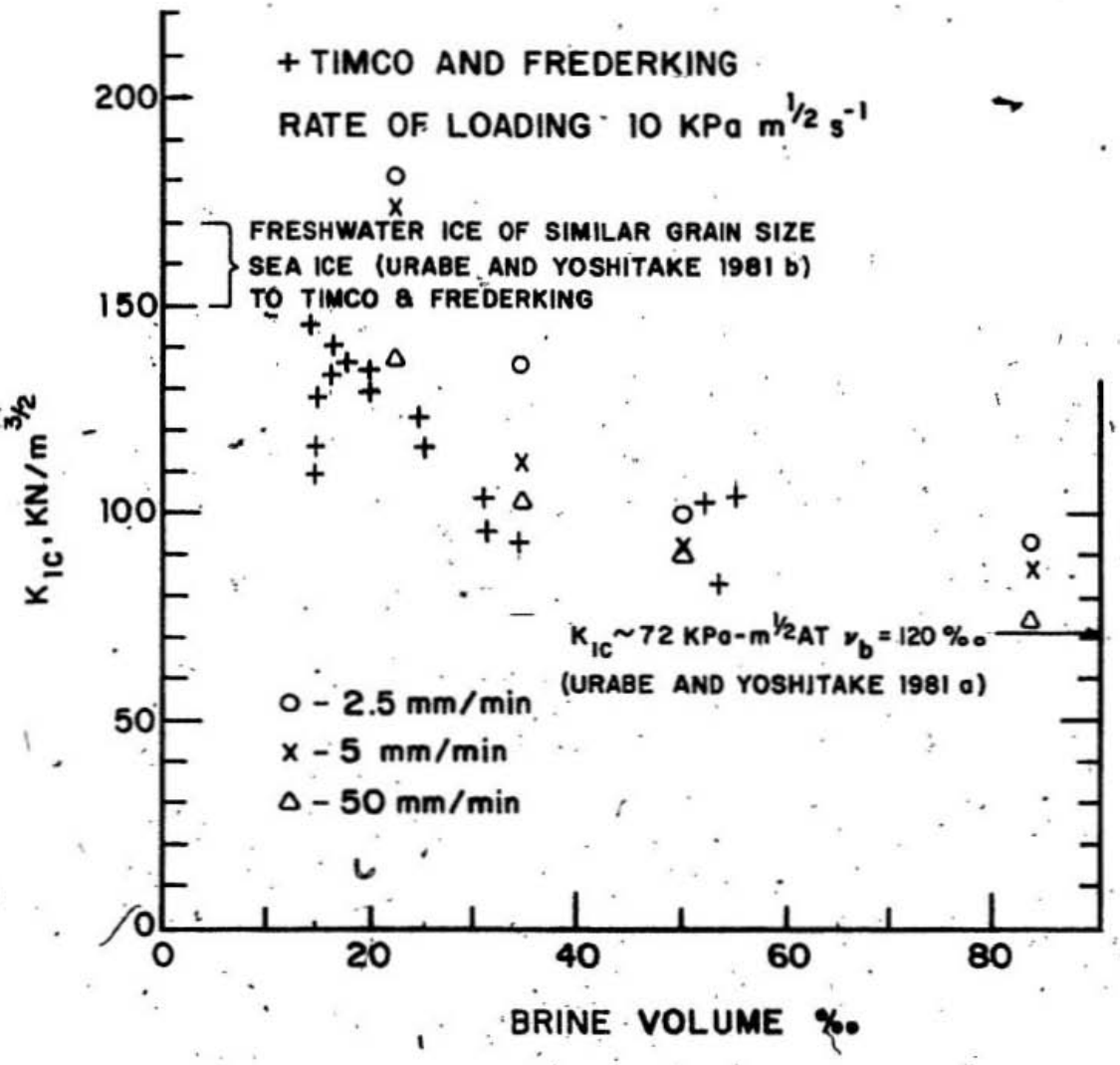

Fig. 19 K_{IC} as a function of Brine Volume

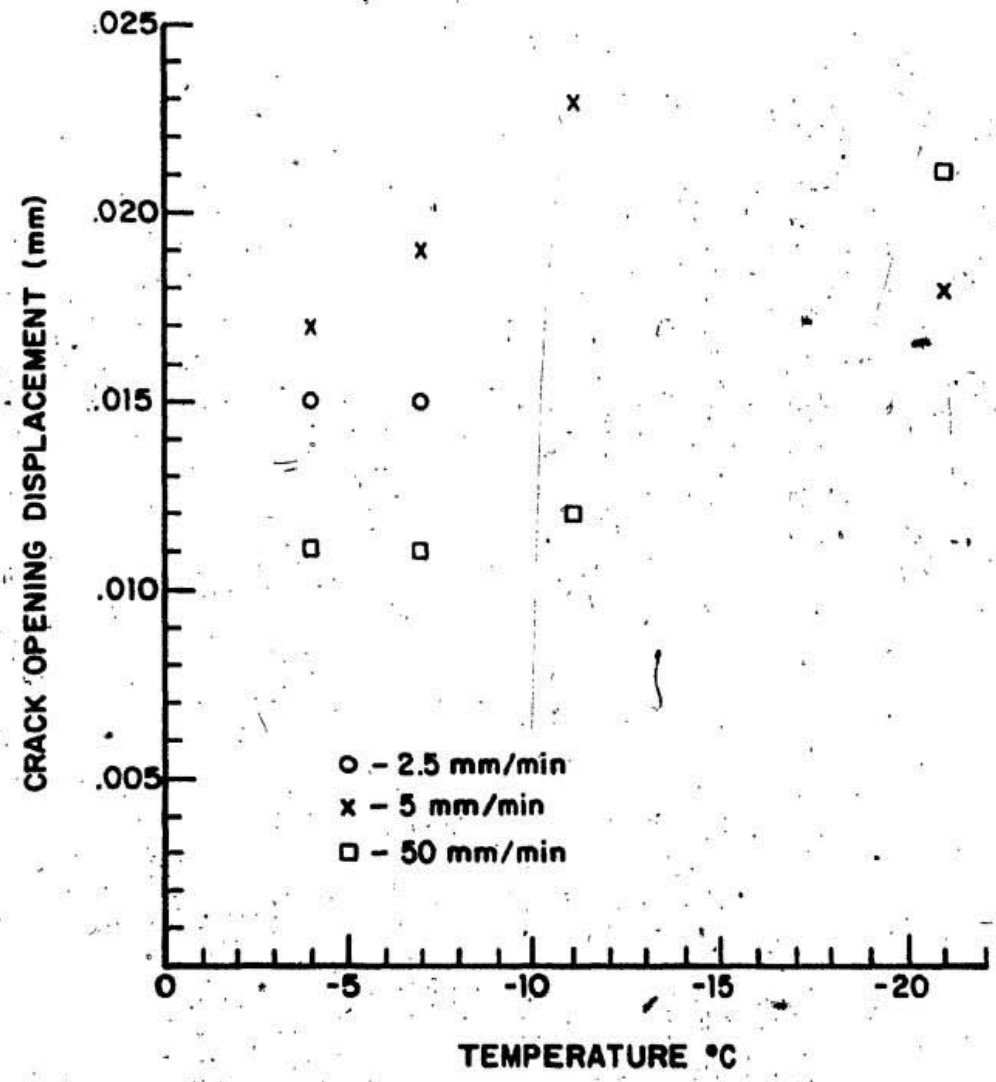

Fig. 20 Critical crack opening displacement for different temperatures

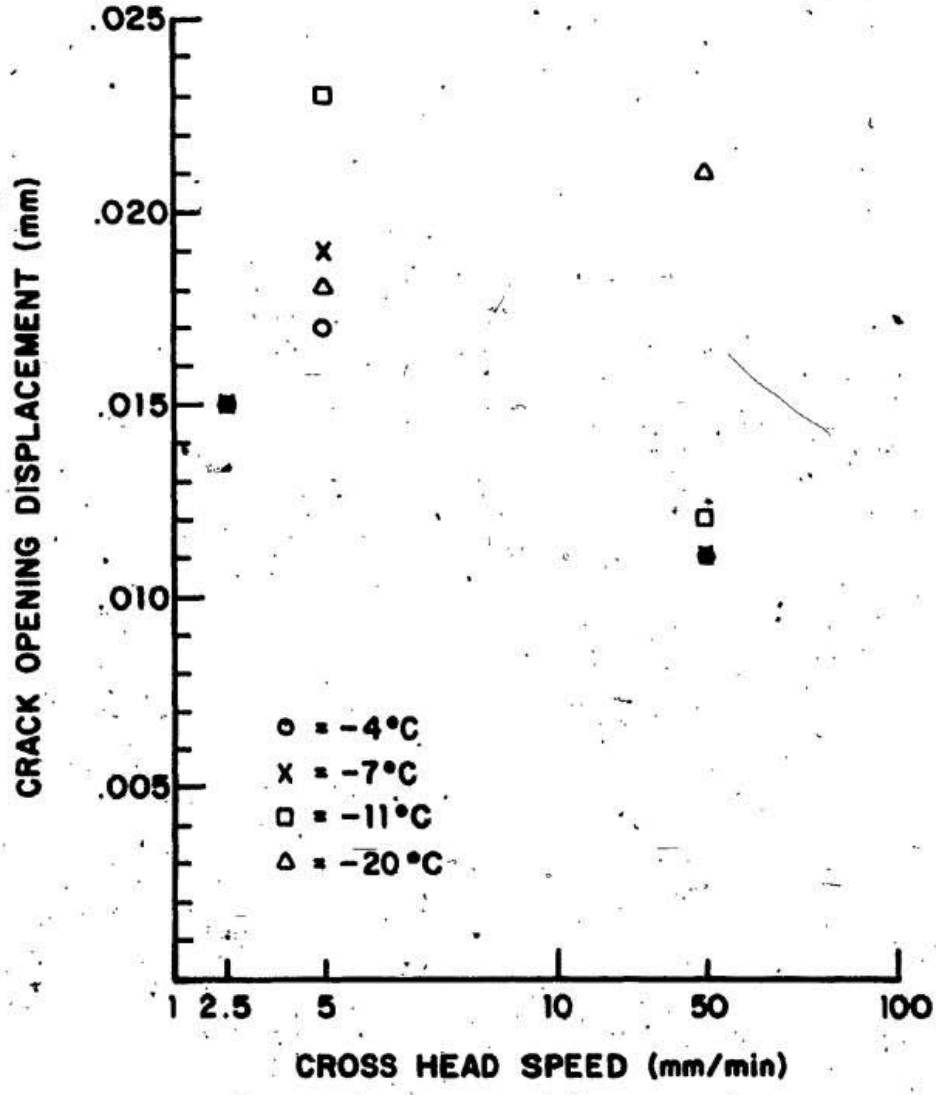

Fig. 21 Critical crack opening displacement for different cross head speeds

APPENDIX

The Freezing of Sea Water

Considering the large number of solid impurities in any small volume of natural sea water, it is almost certain that homogeneous nucleation never occurs. Also in polar regions snow crystals are fairly continuously being deposited on the upper water surface providing nuclei for further growth. The amount of supercooling is probably a few hundredth to tenth of a degree centigrade. In general, the freezing of sea water appears to be similar to that of fresh water and it is reasonable to assume that the first crystal to form will be minute sphere of pure ice (Hobbs, 1974). Growth rapidly changes these spheres into thin circular discs in the general growth sequence spheres - discs - hexagonal dendritic stars. The growth rate of ice is strongly dependent on the growth direction. In ice discoids this plane of maximum growth is the (0001) or basal plane which is the plane of maximum atomic density in an ice crystal. The crystal growth parallel to the c-axis is in the order of magnitude slower than in the (0001) plane and the resulting kinetics are consistent with the classical volume - Stranski models which are based on the assumption that two dimensional nucleation and growth is the rate controlling mechanism. The star-like crystals grow rapidly across the surface of calm sea water until they overlap and freeze together forming a continuous thin ice skim. Because of the tabular nature of both the initial ice discoids and stars,

they float with their basal planes (0001) in the plane of water surface. Ideally this would produce an ice skim with a completely c-axis vertical orientation. However, since water conditions are rarely completely calm a number of discoids or stars are usually caught in an intermediate position i.e. with their c-axis inclined at some angle to vertical. In this skim there is a strong c-axis orientation and a few crystals in other orientations. A study of a number of thin sections under polarized light showed that in this ice-skim commonly >50% of the upper ice surface is composed of crystals with their c-axis approximately vertical.

The formation of a cover of ice on the surface of sea is a refining process in which most of the salt is rejected. The freezing rate is usually too rapid for the rejection to approach completion, however, as the growing ice crystals trap a certain amount of brine, cutting it off from the melt. The quantity trapped is highly variable function of the freezing rate. If the ice cover is broken in the Arctic, and sea water exposed to air temperature of -30° to -40°C the first ice formed may have a salinity S as high as 20°/∞ but for a cover of annual ice a typical average figure is S = 4°/∞, that is almost 90% of the salt is rejected during freezing. The brine retained in the sea ice makes it a very different material from pure ice and we must examine the role of brine in detail, starting with its physical chemistry. Consider first a simple binary system of a solution of sodium chloride in water, which experiences a de-

creasing temperature. The freezing point, or temperature at which ice starts to form, will be depressed below zero as shown in Fig. (22) which is the phase diagram for this binary mixture. Point A represents brine of 35°/∞ salinity at 0°C. It must be cooled to -2.1°C before any ice is formed. Once the solid phase appears, there is a unique temperature at which ice and brine of a given concentration (salinity) can exist in equilibrium. If we cool our sample below -2.1°C it must follow this equilibrium line, to C, where the temperature is -8.5°C and the brine now has S=125°/∞. In other words, exactly sufficient water must freeze so the remaining salt and water form a brine of this salinity. As long as the temperature of the sample remains constant this is a stable equilibrium, but an increase in temperature will result in some melting of ice and conversely. If the temperature lowered still further, a limit is reached at the point E, called Eutectic point. Liquid brine cannot exist below this point, which in the case of sodium chloride brine is at a temperature of -21.1°C with a eutectic composition of 233°/∞ salinity. The dashed part of the curve is of less interest in connection with sea ice. It shows what happens if the initial composition of the brine is more concentrated than the eutectic composition. For example, if we started with a solution with S=250°/∞ this solution could be cooled to -10.4°C and still remain a liquid. Below this temperature, solid salt would be precipated in the hydrated form $NaCl.2H_2O$ and the equilibrium point would follow the dashed curve to E.

Sea Ice Structure

Structurally undeformed first-year sea ice is very similar to a cast ingot. Its uppermost zone (the initial skim) is produced by the formation of the initial ice layer across the sea surface. This layer may vary from a few millimeters to 20 cm in thickness depending on the sea state at the time the ice cover forms. The layer below this can be referred to as the transition zone, in that a preferred growth orientation develops in the crystals. Although these upper two layers are quite interesting from a crystal-growth point of view, they are usually very thin (the base of the transition zone is commonly less than 30 cm below the upper surface of the ice sheet), and do not need to be considered for most engineering purposes.

During the melt season, the upper two layers commonly ablate away causing multi-year ice to be essentially completely composed of ice of the third zone. The ice of this so-called columnar zone characteristically has a strong preferred growth fabric with the crystals elongated vertically parallel to the direction of heat flow and the c-axes of the crystals oriented almost perfectly in the horizontal plane. This results in the basal planes of the ice crystals being oriented in a near-vertical direction. The geometric selection that occurs, as crystals with their c-axis oriented close to horizontal cut out other less fortunately oriented crystals, causes a gradual increase in grain size with depth at least in the upper portion of the ice sheet. In fact the very limited number of measurements of grain size (Weeks and Assur, 1967) suggested that the mean crystal diameter increases with depth at a rate independent

of the grain size present at the base of the transition zone. Because the size of the crystals becomes large relative to that of the samples usually taken, adequate descriptions of grain-size variations are only available for the top 60 cm of first-year ice. Limited observations of the lower portions of 2 m thick ice show large areas (at least 1 m in diameter) that have roughly colinear c-axis orientations (Peyton, 1966). Although the degree of colinearity is not sufficient for such areas to be considered as single crystals, the degree of preferred orientation would clearly result in large variations in physical characteristics such as ice strength with changes in the direction of loading.

Each individual crystal of sea ice is sub-divided into a number of ice platelets that are joined together to make a sort of quasi-hexagonal network as viewed in the horizontal plane. It is within this network that most of the entrapped brine present in the sea ice is believed to be located.

The Variation of Salinity with Time

Sea ice in nature is virtually never in an equilibrium state. We shall see that most of its physical properties depend on the brine content ν, and this parameter varies with time because of both temperature and salinity changes. The salinity of sea ice changes in two ways. At least at temperature above -15°C, the brine cells have some interconnections so that brine may drain slowly through the ice under the influence of gravity. A piece of sea ice cut out from an ice cover stored at -15°C or higher, gradually "bleeds" brine, the rate of discharge of the brine increasing rapidly with temperature as the brine cells become enlarged.

If there is any temperature gradient in sea ice (as is virtually always the case), the brine cells migrate along the gradient in the direction of higher temperature. In Fig. 25 consider a long vertical brine cell, and the usual temperature condition, namely that the ice-air interface is colder than the bottom of the ice sheet, which is fixed at the freezing point of the sea water. Because of diffusion the concentration of brine within the cell will be uniform, and of a salinity to match the mean temperature of the ice surrounding the cell. Hence at the warmer end the brine is too concentrated and will dissolve ice to reduce its concentration. At the colder end more ice freezes to increase the brine concentration and the net effect is to move the entire cell of brine along the gradient. In a sea ice cover the brine migration

acts in the same direction as brine drainage so that the two effects are additive. Both processes take place slowly, but at a measurable rate, in an ice cover during the winter months. Brine drainage is quite rapid when the ice approaches its melting point. If a block of ice is removed from contact with the sea, as by being pushed up on shore, it loses salt very rapidly during the warmer months of spring and summer.

Consider now the state of an annual ice floe in the Arctic Ocean which does not melt completely during the brief and cold summer. For a period of a month or so it is at an almost uniform temperature only slightly below its freezing point. The brine cells are enlarged, and so interconnected with each other and the sea that the ice sheet is saturated with sea water; a hole dug in a floe in summer fills with sea water up to the hydrostatic level in a matter of seconds. This sea water is presumably in the channels in the ice which the brine cells formed, and the effect is to replace the concentrated brine of the winter ice by sea water of normal salinity without a proportional increase in the size of the brine cells. Since this is what happens, it is clear that the various processes of ice melting, brine drainage, and diffusion are <u>not</u> taking place in thermodynamic equilibrium. When the temperature of the ice drops again, brine cells get cut off from each other and from the sea, and decrease in size to smaller diameters than they had the previous winter. The floe is now called polar ice and its salinity is much lower than that of annual ice. This

removal of salt from sea ice may continue during a second summer; this is not certain, but in any event most of it is removed during the first year. Recently Pounder compared ice known to be about eighteen months old with several-year-old polar ice. Their salinities were 1°/₀₀ and 0.5 °/₀₀ respectively, in contrast with the typical 4°/₀₀ of annual ice. The Eskimos have long known that potable water can be obtained by melting sea ice which is over a year old.

Young's Modulus for Sea Ice

Values of Young's modulus for fresh water ice have been reported in the range of 3×10^6 to 11×10^6 kPa with a few exceptions. These values have been obtained by static methods such as the deflection or extension of a beam under load. Due to the visco-elastic nature of the ice, there is a large scatter in the results. The Young's modulus of ice is more reliable if dynamic methods of testing are used.

Data on the elastic moduli of sea ice are few. M.P. Langleben used the dynamic method for determination of Young's modulus of sea water over a wide range of salinities (ice from 4 to 24°/$_{oo}$) and also temperatures (-3 to -26°C). He reported the modulus of elasticity to be a function of brine volume

$$E = (10.00 - 35.1v) \times 10^{10} \text{ dyne/cm}^2$$

The energy release rate (G) and yield stress (σ_y) was calculated, in this work, by means of the same formula. A value of Poisson's ratio of 0.3, as reported by Langleben, was also used.

Crack-Tip Stress And Strain Fields

In general the crack tip can be divided into three separate zones as in Fig. 23.

They are (1) elastic, (2) elastic-plastic and (3) an intensely nonlinear (large strains and rotations) zone.

The elastic zone (1) may be appropriately used only if the crack tip plastic zone is small compared to planar distances to other boundaries (or load points). That is to say for small scale yielding Linear Elastic Fracture Mechanics (LEFM) is appropriate to yield values of K_{1c}. An elastic-plastic zone (2) must be adopted for the so called elastic-plastic fracture mechanics regime. However, we must remain aware of the limitation that the intensely nonlinear zone (3) should then remain small compared to planar distances to the boundaries. Now if zone (3) is comparatively small, then zone (2) may be regarded as an elastic-plastic field surrounding the crack tip (which is a non linear zone), which lends itself to analysis by the usual plasticity theories. It is emphasized that this viewing procedure is completely analogous to LEFM wherein if the whole plastic zone is comparatively small, then view (1) may be regarded as linear elastic field, surrounding the crack tip, which lends itself to analysis by the theory of elasticity.

Linear-Elastic Crack-Tip Stress and Strain Field

Viewing the plastic zone as small compared to the extent of surrounding elastic material, linear elasticity is applied to obtain the elastic field equations surrounding the near neighbourhood of the crack tip. The distribution of stresses σ_{ij} and strain ε_{ij} have the characteristic of $1/\sqrt{r}$ singularity (higher order terms have been ignored). The analysis for this zone is through the usual LEFM theory, and K is the parameter describing the intensity of the field. K is thus determined from loads and body dimensions including crack size using the solution of an elastic boundary value problem for the configuration of interest.

Elastic-Plastic Crack Tip Stress and Strain Fields

The fully elastic-plastic zone (2) is illustrated in Fig. 24. The view is taken that an elastic-plastic field (with small strains and rotations) surrounds the crack tip within the region denoted by (2), but outside the intensely non linear zone. Using plasticity theory Hutchinson obtained the form of the stress, σ_{ij}, and strain, ε_{ij}, fields

$$\sigma_{ij} = \sigma_o \left(\frac{J}{r\,\sigma_o\,\varepsilon_o}\right)^{\frac{N}{1+N}} \tilde{\Sigma}_{ij}(\theta,N)$$

$$\varepsilon_{ij} = \varepsilon_o \left(\frac{J}{r\,\sigma_o\,\varepsilon_o}\right)^{\frac{1}{1+N}} \tilde{E}_{ij}(\theta,N)$$

If $\bar{W} < r <<$ planar dimensions, ($\bar{W}$ is defined in Fig. 24).

Thus J is seen to be an equivalent field parameter to its analog K, and the LEFM analysis is extended fully into the elastic plastic regime by the J integral as well as crack opening displacement (C.O.D.). These two methods are used for the calculation of the elastic plastic (2) zone.

Definition of the J integral

The energy line integral, J, is applicable to elastic material or elastic-plastic material when treated by a deformation theory of plasticity. It is defined for two-dimensional problems and is given by the equation

$$J = \int_{\Gamma} W dy - T \left(\frac{\partial u}{\partial x}\right) ds$$

As illustrated in Fig. 24, Γ is any contour surrounding the crack tip. The quantity W is the strain energy density

$$W = W(\varepsilon_{mn}) = \int_{o}^{\varepsilon_{mn}} \sigma_{ij} \, d\varepsilon_{ij}$$

T is the traction vector defined by the outward normal n along Γ, $T_i = \sigma_{ij} n_j$, u is the displacement vector and s is the arc length along Γ.

Since paths can be chosen close to the crack tip, the energy line integral represents some average measure of the near tip deformation field.

Since the path independent J integral is a field parameter, the J_{1c} fracture criterion is compatable with any criterion based on features specific to the crack tip region. There is no discrepancy between the J_{1c} approach and fracture criteria based on C.O.D.

Simple compliance type experiments can be used to determine the value of the J integral. As with the COD value, J_{1c} is simply related to the parameters of linear elastic fracture mechanics

$$J_{1c} = G_{1c} = \frac{1-\nu^2}{E} K_{1c}^2$$

Crack Opening Displacement (COD)

The fracture behaviour in the vicinity of a sharp crack could be characterized by the opening of the notch faces - namely the crack opening displacement (COD). It has been shown that the concept of COD is analogous to the concept of critical crack extension force (G_c), and thus the COD values could be related to the plane strain fracture toughness K_{1c}. Because COD measurements can be made even when there is considerable plastic flow ahead of a crack, such as would be expected for elastic-plastic or fully plastic behaviour. The energy release rate (G) can be calculated by using equation

$$G = \frac{K_{1c}(1-\nu^2)}{E}$$

The crack opening displacement is related to the displacement measured on the face of the specimen, δ_m by the expression

$$\delta = \frac{\delta_m}{1 + \frac{2.7(a+z)}{h-a}}$$

where z is the height of the knife edge supporting the gauge above the ice surface, a the crack length, and h the specimen width. The displacement at the crack tip is related to the yield stress in the plastic zone by the expression

$$\delta = K_{1c}^2 \frac{(1-\nu^2)}{E} \cdot \frac{1}{\sigma_y} = \frac{G}{\sigma_y}$$

Therefore the energy release rate (G) and yield stress of ice (σ_y) could be calculated by knowing the stress intensity factor K_{1c} and the crack opening displacement C.O.D.

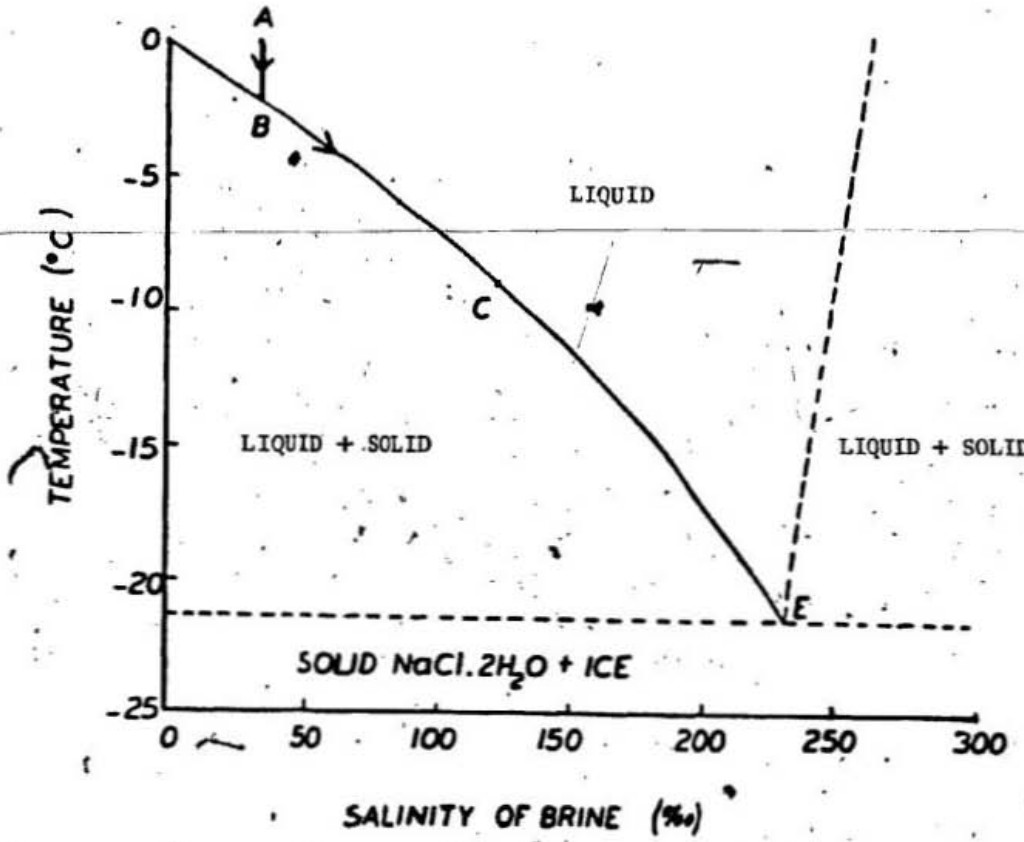

FIG. 22 The phase diagram of a binary system consisting of NaCl and H_2O. Eutectic temperature is −21·1°C.

(From Pounder, 1965)

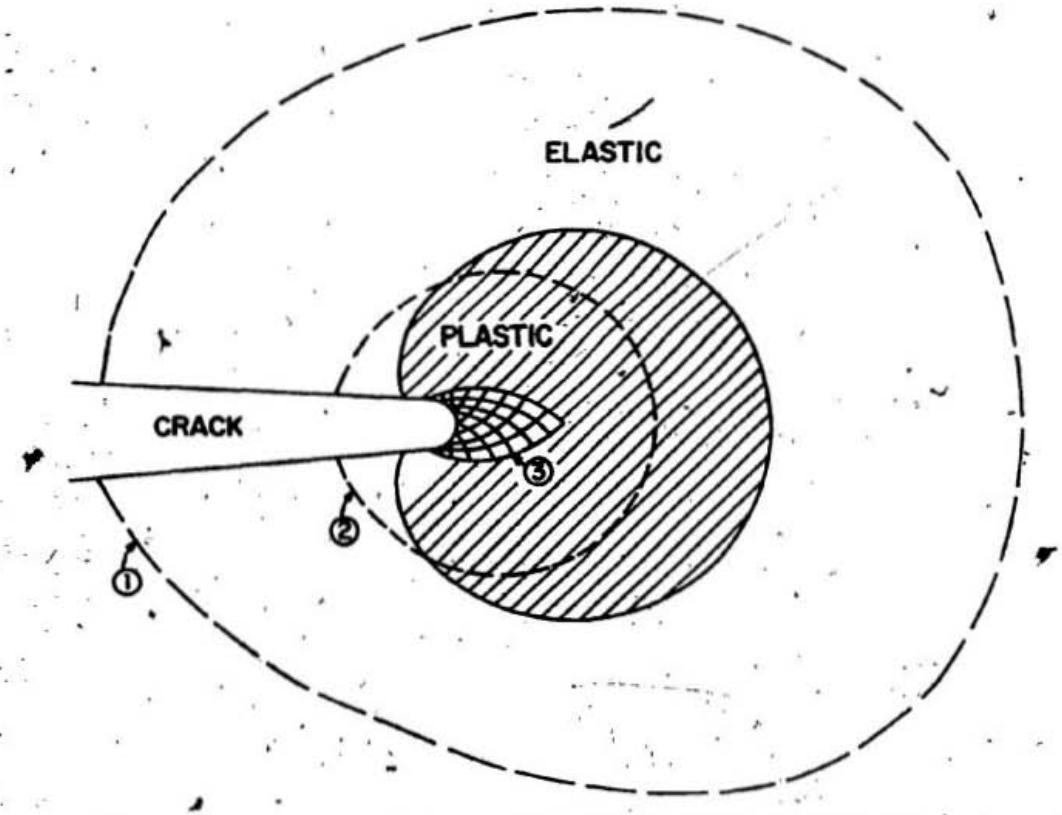

VIEW ①: AN ELASTIC FIELD SURROUNDING THE CRACK TIP.
VIEW ②: AN ELASTIC-PLASTIC FIELD SURROUNDING THE CRACK TIP.
VIEW ③: AN INTENSE ZONE OF DEFORMATION.

FIG.23. Crack-tip stress and strain fields surrounding the crack tip.
(From ASTM STP 631)

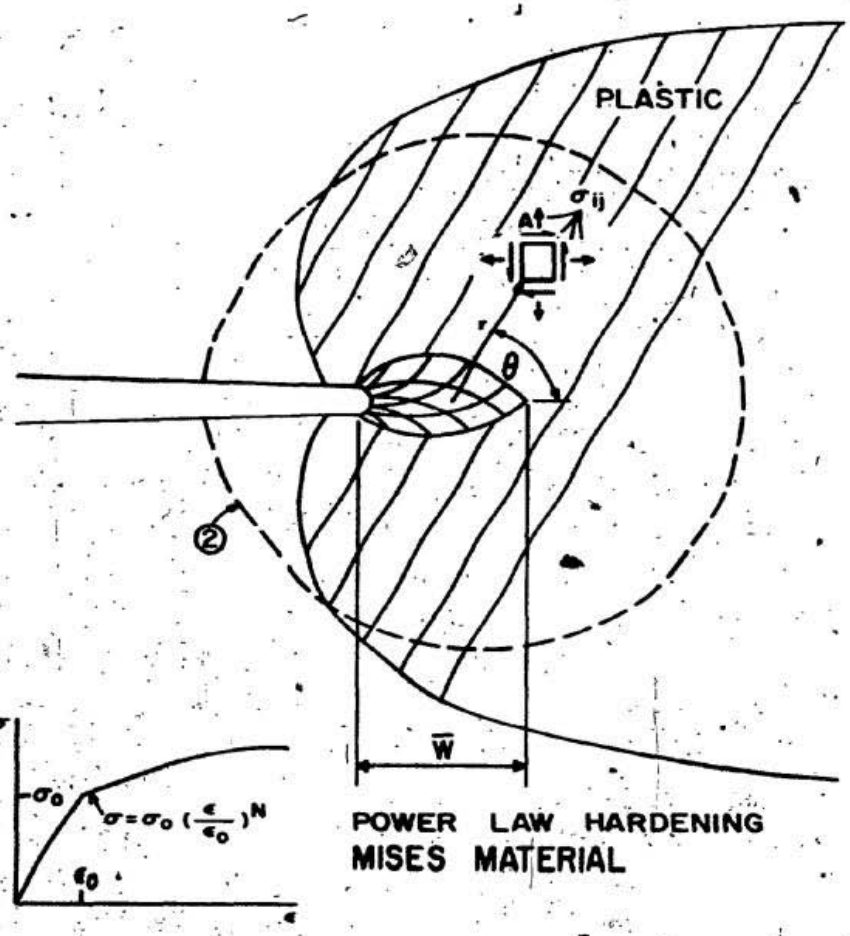

FIG.24. Elastic - plastic crack - tip stress and strain fields.
(From ASTM STP 631)

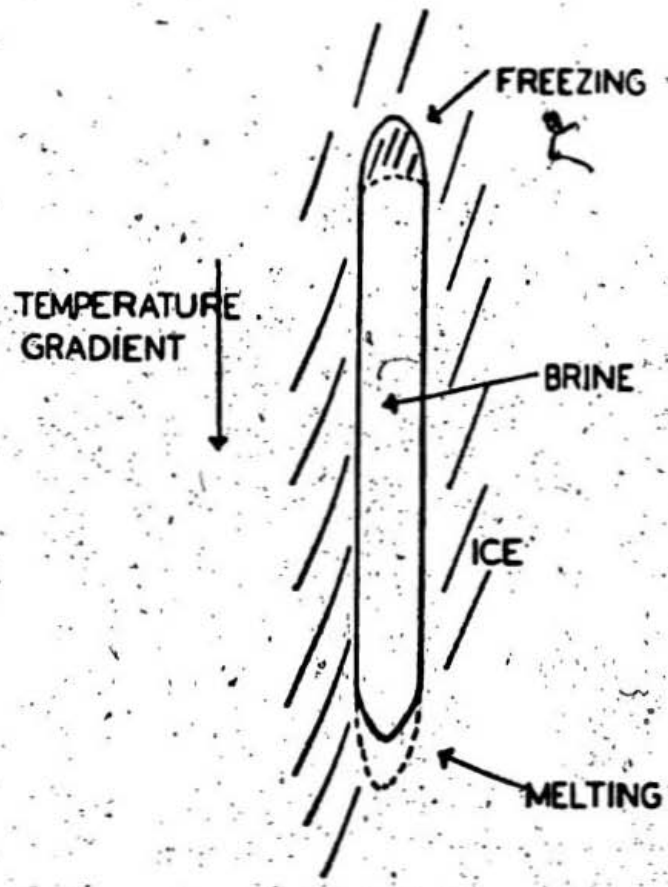

FIG. 25 **Brine migration along the temperature gradient.**
(From Pounder 1965)